NASA-CR-203759

Development of Advanced Methods of Trajectory and Structural Analysis for Hypersonic Aircraft

Final Report

Dr. Mark D. Ardema
Principal Investigator

October 1, 1995 - January 31, 1997

Santa Clara University
Santa Clara, CA 95053

NASA Ames Research Center Grant NCC2-5165

Introduction

This report summarizes work accomplished under NASA Grant NCC-5165, "Development of Advanced Methods of Trajectory and Structural Analysis for Hypersonic Aircraft" from October 1, 1995 to January 31, 1997. The effort was in two areas: (1) development of advanced methods of flight path optimization, and (2) development of advanced methods of structural weight estimation.

During the Spring of 1996, both graduate student research assistants working on the project, H.C. Chou and Mark Chambers, resigned to take positions in industry. This required assigning three new Santa Clara people to the project: Dr. Lee Hornberger, associate professor of mechanical engineering; Robert Windhorst, graduate student research assistant; and Frank Dickerson, undergraduate student. These new people inevitably required time to learn the HAVOC code and the nature of the ongoing research. The result was that completing the tasks in the work statement required an extension of the Grant beyond the original termination date.

M. Green and J. Bowles were the NASA collaborators on the Grant.

Review of Results in Flight Path Optimization

A paper on the operation of air-breathing propulsion, prepared under a previous grant, was accepted and published during the past year: "Near-Optimal Propulsion-System Operation for an Air-Breathing Launch Vehicle", M. Ardema, J. Bowles, and T. Whittaker, Journal of Spacecraft and Rockets, Vol. 32, No. 6, Nov-Dec 1995, Pp 951-956.

A paper on the optimality of dual-fuel rocket engines, prepared and submitted under a previous grant, has been accepted and published during the past year: "Near-Optimal Operation of Dual-Fuel Launch Vehicles", M. Ardema, H. Chou, and J. Bowles, Journal of Guidance, Control, and Dynamics, Vol. 19, No. 5, Pp 1180-1182. Also, a more extensive paper on the same subject was presented at a technical conference. The main results of the dual-fuel study were that dual-fuel rockets have better performance than do single-fuel, and that the optimum transition Mach number between dual-fuel and single-fuel modes is about 9. The details may be found in the conference paper, included here as Appendix A.

The main area of work in the trajectory area was the optimization of re-entry flight paths. When maximum turn angle and maximum cross-range trajectories were attempted, a fundamental problem was discovered. This necessitated a basic investigation of energy-state and related approximations. The results of this analysis are found in Appendix B, and will be briefly reviewed here.

The analysis in Appendix B shows that for the problem of maximizing heading angle change, the energy-state approximation does not reduce the problem to a function optimization, as opposed to a functional one, that is, the $\dot{E}$ and $\dot{\chi}$ equations remain coupled. The coupling occurs in the earth curvature (centripetal) terms and in the earth rotation (Coriolis) terms. Although the latter are relatively small effects, the centripetal terms are relatively large at the start of re-entry from orbit. If both of these types of terms are ignored, a simple algorithm for the optimal controls results. For the problem of maximizing cross-range, the problem is more serious because there is coupling in addition to the curvature and rotation terms. This issue will require further investigation.

The major task of the project was to obtain re-entry trajectories under a variety of performance goals: minimum time, minimum temperature, minimum heating, and maximum heading change. As just mentioned, the maximum heading change results must be viewed as suspect at this point.

Figures 1-6 illustrate minimum time re-entry trajectories. Although these are not of direct interest, they are useful for demonstrating energy-state trajectories and provide a benchmark for comparison with later results. Four classes of trajectories were investigated: no banking, optimal left turn banking, optimal right turn banking, and optimal bank chattering. These latter assume infinitely fast reversals of bank angle such that the net effect on the ground path is zero.

Figure 1 shows that the ground path is considerably shortened if banking or chattering is allowed, and Figure 2 shows that banking shortens the re-entry time by about 200 seconds. Figure 3 shows that the banking trajectories have much lower dynamic pressure than does the non-banking one, and Figure 4 shows that the angle-of-attack of the banking trajectories is much higher than for the non-banking ones. The bank angle of the banking trajectories is in the range of 60° - 80° (Figure 5). Figure 6 shows the history of the temperature at a point on the windward side of the vehicle ⅓ of the way back from the nose. For all the minimum time trajectories, this temperature is 1900°F (the upper limit imposed) for a significant portion of the trajectory. All these minimum time results seem to make good physical sense.

The minimum temperature (⅓ back on windward side) trajectories are shown on Figures 7-12. Comparison with the minimum time paths of Figures 1-6 show significant differences. The minimum temperature trajectories are significantly longer in both range and time (5300 n.mi. down range as compared with 1700 n.mi. at most, 2000 sec. as compared with 500 sec.); they have relatively low dynamic pressure. When allowed to bank or bank-chatter, there is a little banking at the end, where temperature is not a factor; at high speeds, there is no banking, which is to be expected. The maximum temperature is greatly reduced relative to the minimum time paths (1400°F as compared with 1900°F) and the time at high temperature is significantly reduced.

One of the key objectives of a re-entry trajectory is minimizing heat input into the thermal protection system. As a preliminary step, the heat input has been approximated as the integral of vehicle surface temperature over time. Thus the minimum heating trajectories would be expected to be in some sense between the minimum time and the minimum temperature ones. Figures 13-18 show, in fact, that the minimum heating ones are almost identical to the minimum time ones. Of course, it may be that the temperatures on these trajectories are too high for insulation materials.

Trajectories minimizing the integral of temperature to the fourth power over time were also generated. These trajectories, not shown here, were intermediate between the minimum time and minimum temperature ones in terms of both time and temperature.

Maximum heading angle change trajectories are shown on Figures 19-24. The interest in turning trajectories arises from abort requirements, particularly the need to return to the launch site after one orbit. Since turning increases vehicle surface temperatures, this abort trajectory is the case that sizes the thermal protection system. What is desirable is a flight path that results in sufficient cross-range while minimizing heating subject to temperature limits on the vehicle surface. As mentioned earlier, maximum cross-range problems do not reduce to function optimization under energy-state approximation, and therefore maximum heading change trajectories are determined instead as an approximation. (When heading change reaches 90°, it is held constant.) Although there is coupling between the $\dot{E}$ and $\dot{\chi}$ equations for maximum cross range, it is only through the centripetal and Coriolis terms, as mentioned earlier.

Figure 19 shows the ground paths for left and right maximum heading change trajectories, as well as for a nominal zero bank trajectory. Because of the earth curvature and the use of curvilinear coordinates, the nominal trajectory has a curved ground path. The right and left turning trajectories are quite different. The left turning one is a relatively hard turn that is quite different from the nominal. It begins at high angle-of-attack, about 30°, and then switches to about 15° (Figure 22); the bank angle is at 60° - 70° for most of the flight (Figure 23).

In contrast, the right turn is relatively mild and similar to the nominal. The angle of attack is about 15° everywhere and the bank angle is about 40° for the first portion of the flight and zero thereafter. The right hand turn takes considerably more time than the left (Figure 20). For both trajectories, the surface temperature is at the 1900°F limit for a considerable time (Figure 24). It is of interest to note that 15° is the angle-of-attack for maximum lift-to-drag ratio. Thus these trajectories are largely flown at maximum L/D. This is in agreement with the classical result that maximum range in gliding flight is attained at maximum L/D.

The above results approximate the heat input into the vehicle as the integral of surface temperature over time. Midway through the Grant, a task was added to do a more complete analysis of the heat input at a selected location on the surface of the vehicle. This analysis does a heat balance at the vehicle surface and then numerically solves the

one-dimensional heat equation to get the temperature distribution through the thermal protection system. This allows calculation of the heat being transferred into the TPS at the vehicle surface. When coupled with the energy-state trajectory optimizer, this allows minimum heating trajectories to be determined. The analysis has been coded for use in HAVOC. A description of the analysis and the resulting HAVOC subroutine may be found in Appendix C, which is a Santa Clara M.S. Thesis. A paper based on this thesis has been submitted to the 1997 AIAA Guidance and Control Conference.

In summary, the detailed heating analysis results showed that optimal re-entry trajectories were of two types - high dynamic pressure (q) and low q. The low q trajectories have lower surface temperatures and higher descent times than do the high q ones. The low q trajectories gave lower maximum structural temperatures but the differences were very small. If TPS materials capable of higher temperatures could be developed, then the high q trajectories become superior.

Because of changing priorities and the unexpected loss of a senior graduate research assistant, the analysis of the altitude jumps in energy-climb paths could not be completed.

Review of Results in Structural Weight Estimation.

The major area in the structures area was the development of an improved method of estimating the weight of body structure made from composite materials. This involved an extensive literature search and the coding of a composite materials properties subroutine. This work is discussed in detail in Appendix D.

Previously in HAVOC, the weight of composite material structures was estimated assuming quasi-isotropic materials, maximum stress failure theory, and smeared structural elements. The current capability accounts for realistic lay-ups of unidirectional fiber/matrix composites and uses a bi-axial strain failure theory. The analysis is currently being integrated into the ACSYNT computer code. When verified there, it will be ready for integration into HAVOC.

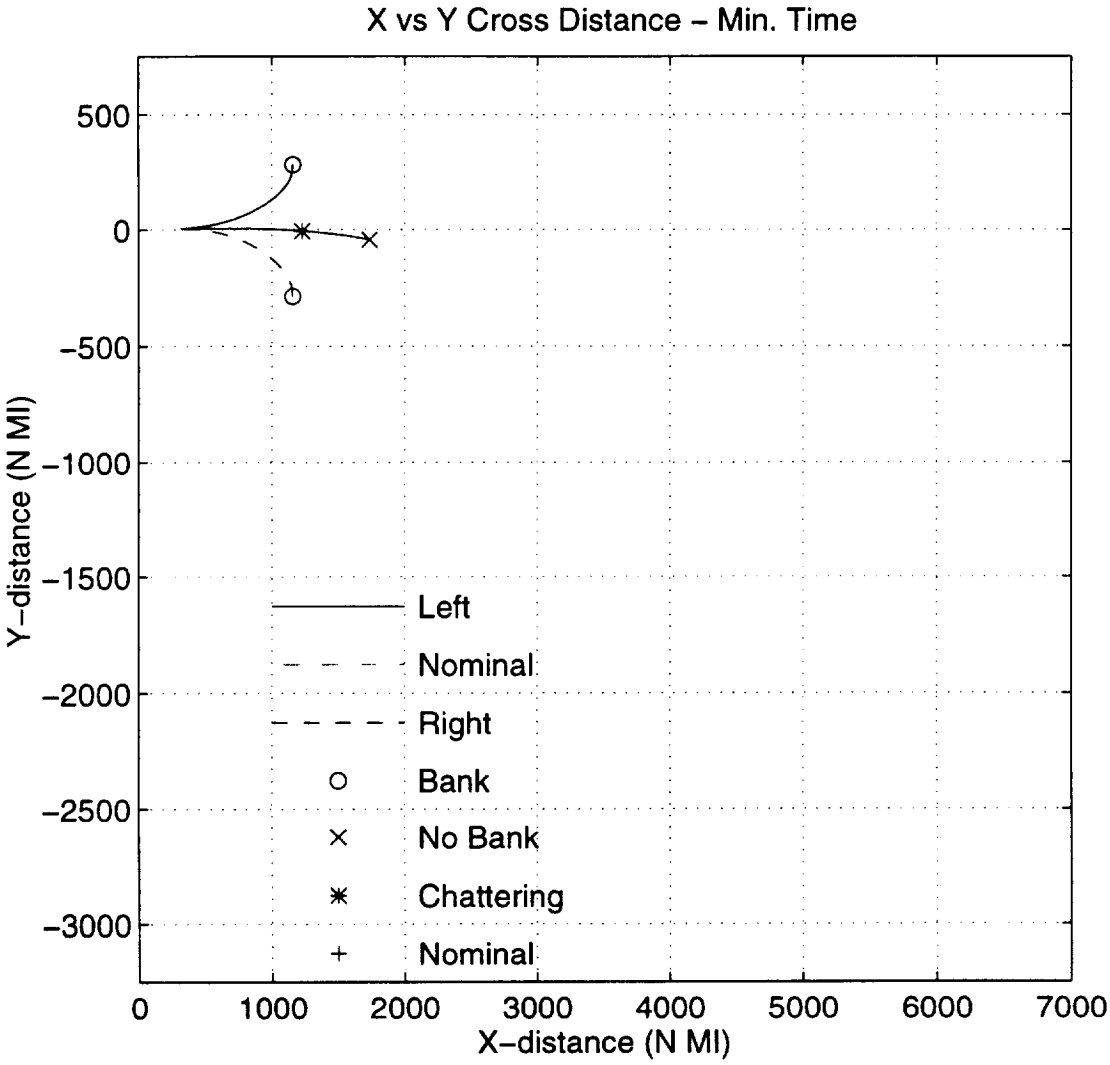
X vs Y Cross Distance – Min. Time
500
0
−500
−1000
−1500
−2000
−2500
−3000
Y−distance (N MI)
0
1000
2000
3000
4000
5000
6000
7000
X−distance (N MI)
Left
Nominal
Right
Bank
No Bank
Chattering
Nominal

Figure 1

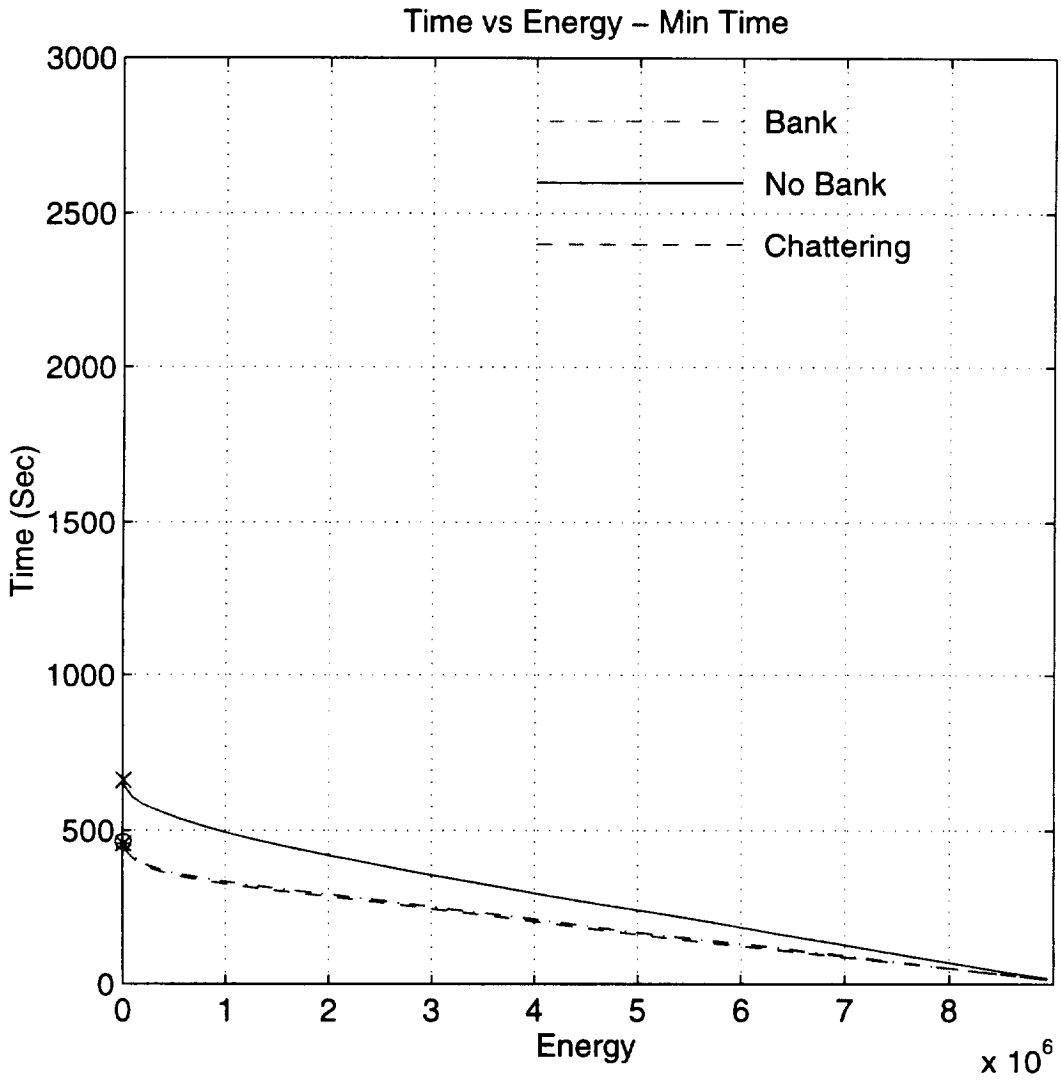
Time vs Energy – Min Time
Bank
No Bank
Chattering
Time (Sec)
Energy
x 10^6
3000
2500
2000
1500
1000
500
0
0
1
2
3
4
5
6
7
8

Figure 2

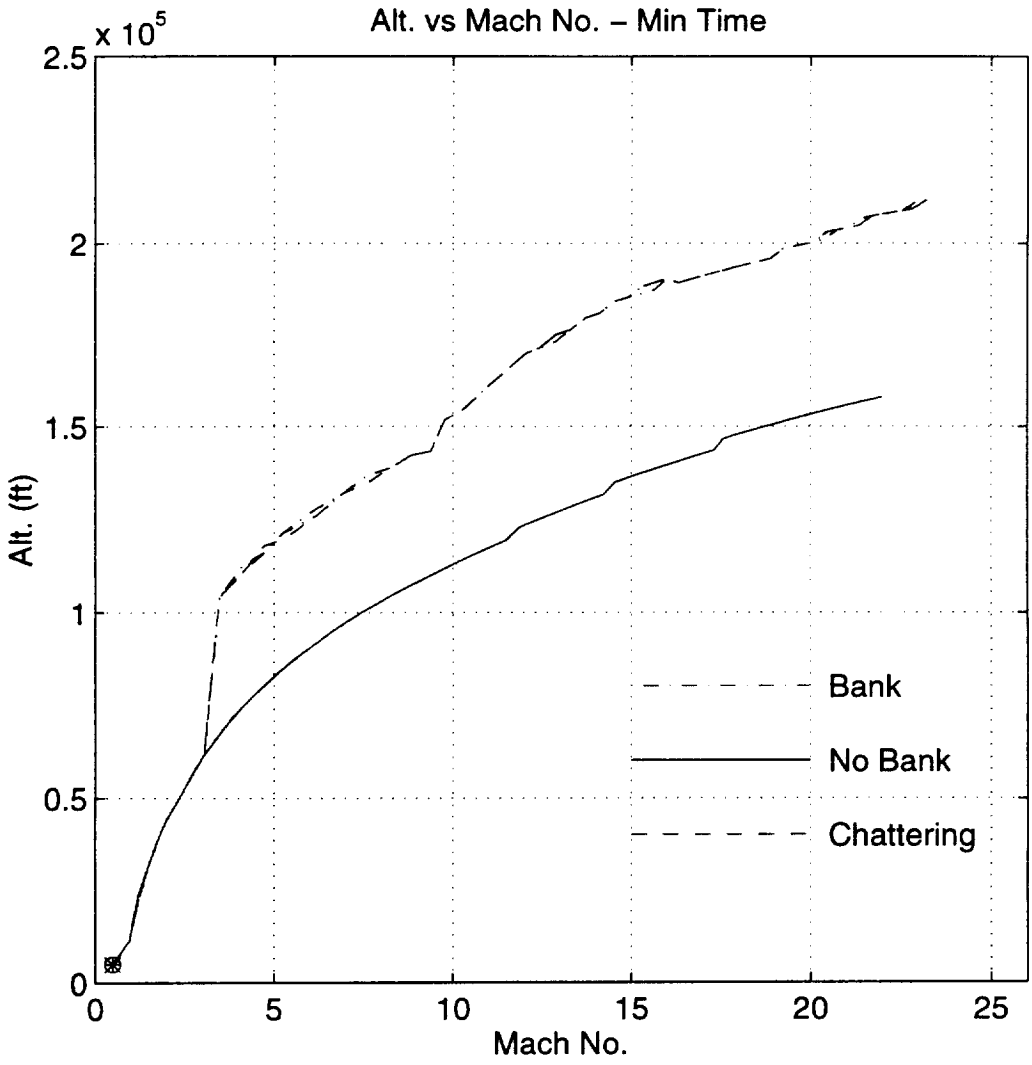
Alt. vs Mach No. – Min Time
x 10^5
2.5
2
1.5
1
0.5
0
Alt. (ft)
0
5
10
15
20
25
Mach No.
Bank
No Bank
Chattering

Figure 3

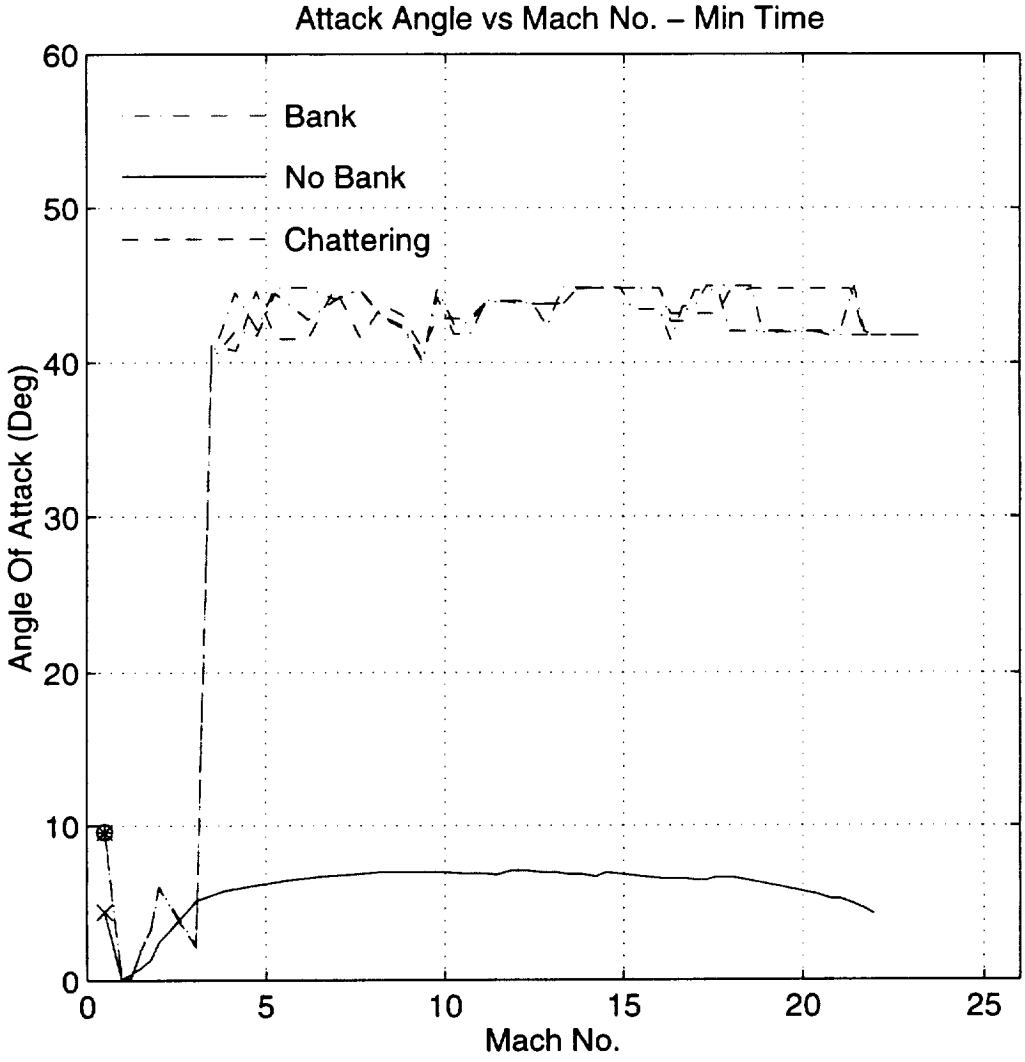
Attack Angle vs Mach No. – Min Time
Bank
No Bank
Chattering
Angle Of Attack (Deg)
Mach No.
0
10
20
30
40
50
60
0
5
10
15
20
25

Figure 4

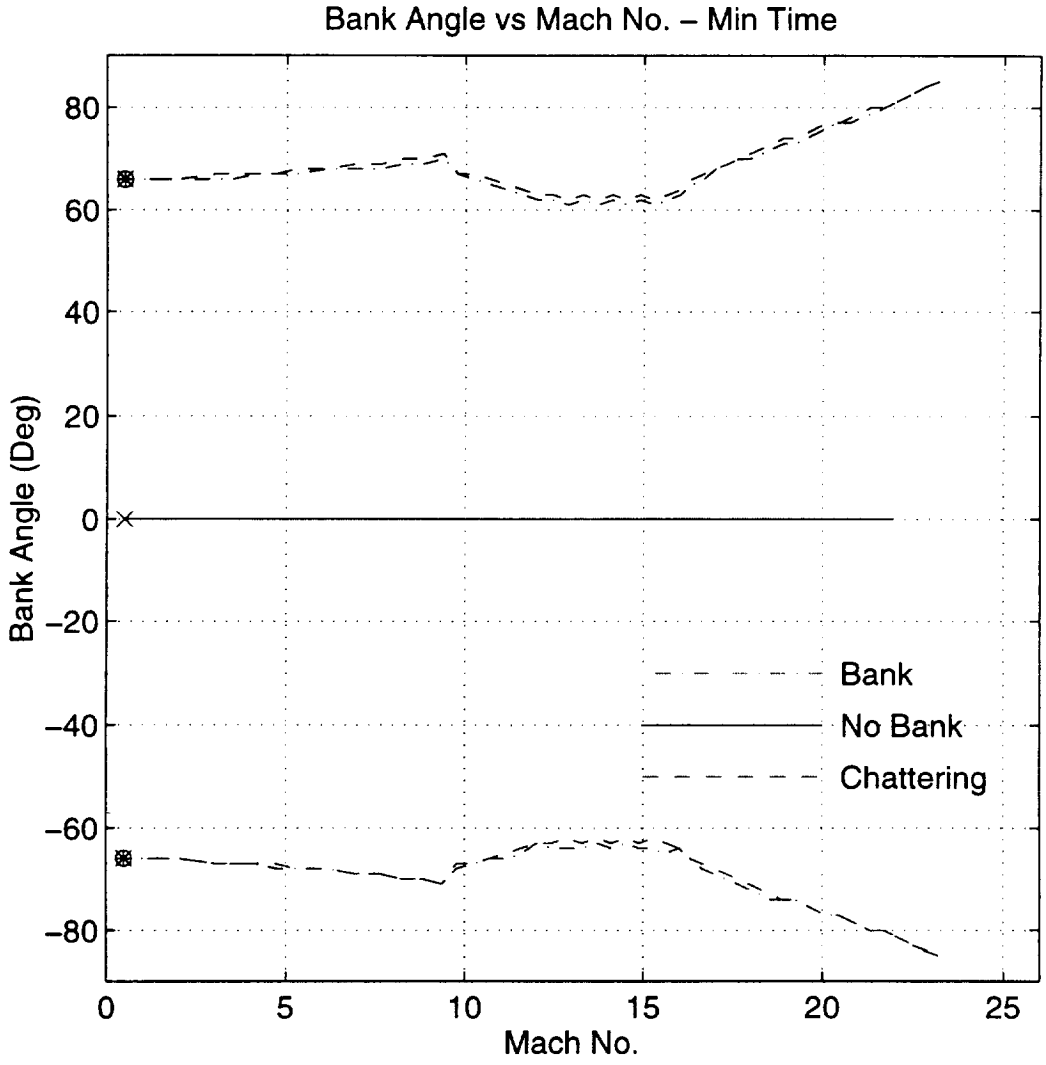
Bank Angle vs Mach No. – Min Time
Bank Angle (Deg)
80
60
40
20
0
−20
−40
−60
−80
0
5
10
15
20
25
Mach No.
Bank
No Bank
Chattering

Figure 5

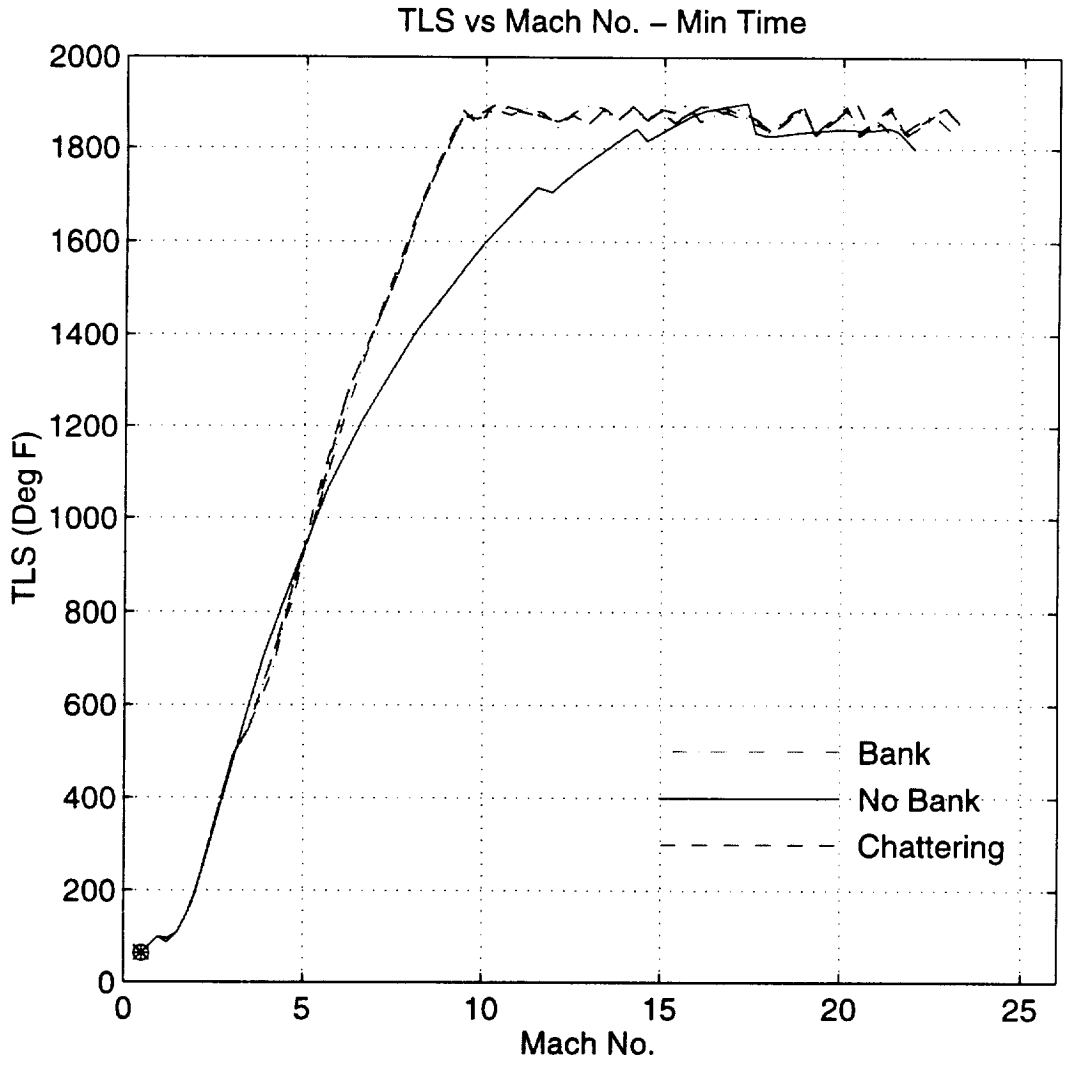
TLS vs Mach No. – Min Time
TLS (Deg F)
Mach No.
2000
1800
1600
1400
1200
1000
800
600
400
200
0
0
5
10
15
20
25
Bank
No Bank
Chattering

Figure 6

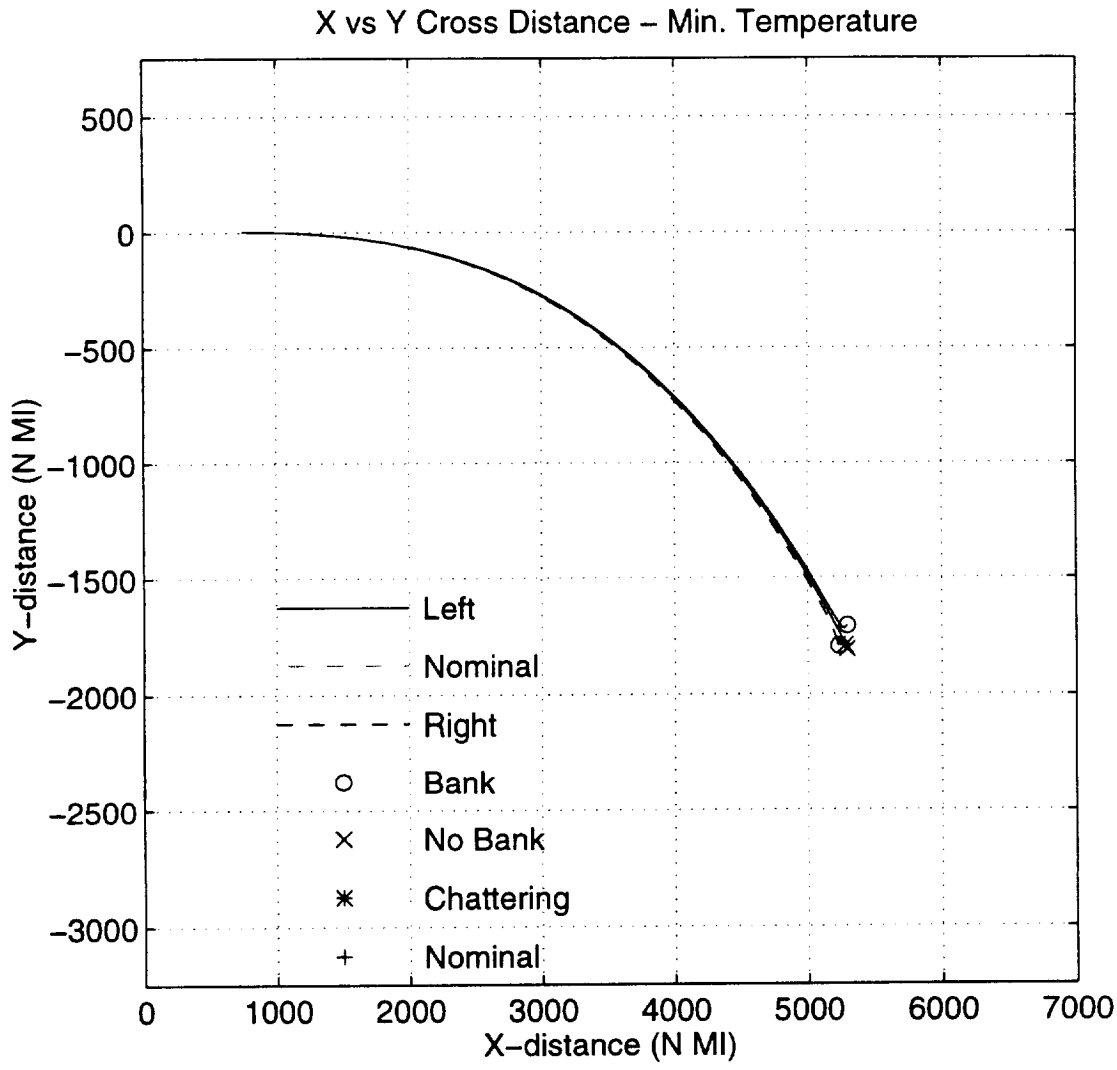
X vs Y Cross Distance – Min. Temperature
500
0
−500
−1000
−1500
−2000
−2500
−3000
Y−distance (N MI)
0
1000
2000
3000
4000
5000
6000
7000
X−distance (N MI)
Left
Nominal
Right
Bank
No Bank
Chattering
Nominal

Figure 7

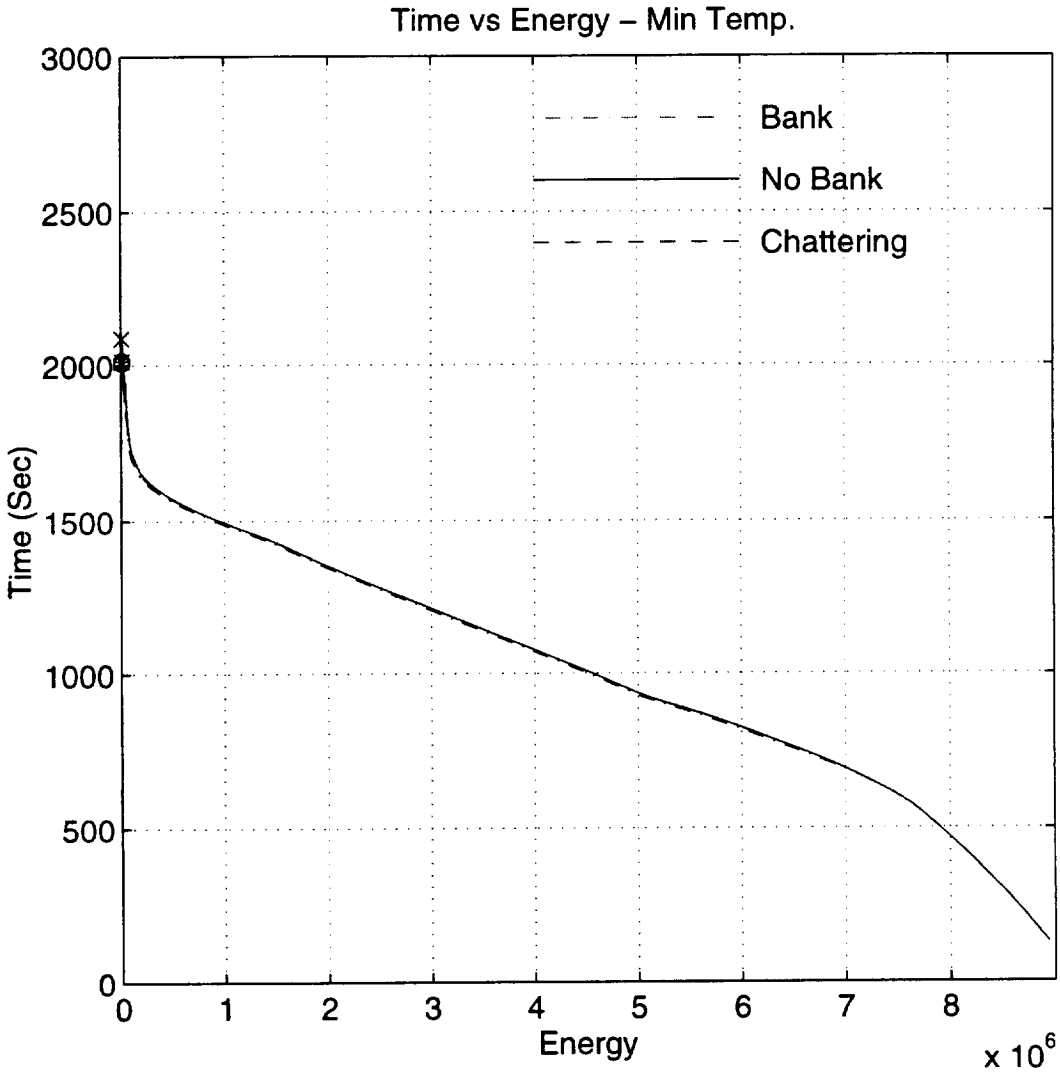
Time vs Energy – Min Temp.
Bank
No Bank
Chattering
Time (Sec)
Energy
x 10^6
3000
2500
2000
1500
1000
500
0
0
1
2
3
4
5
6
7
8

Figure 8

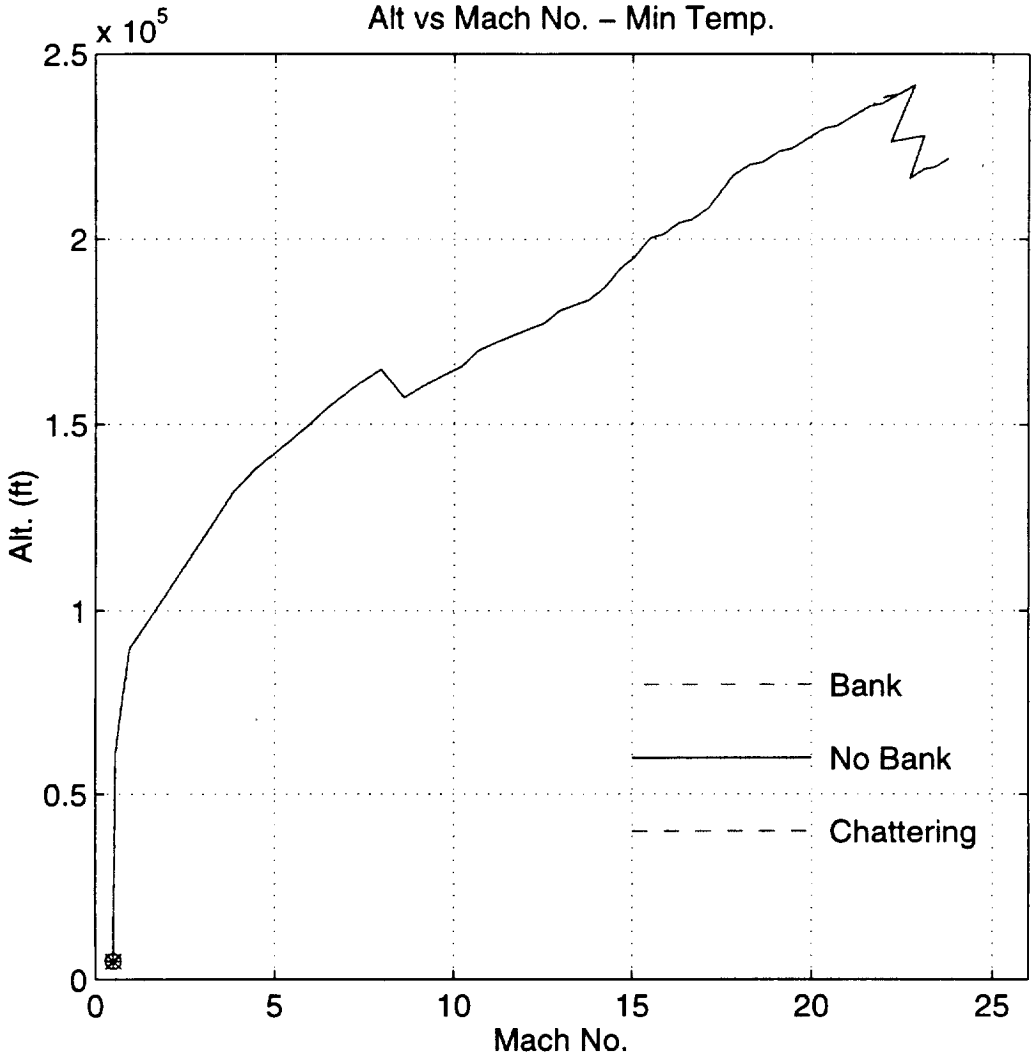
Alt vs Mach No. – Min Temp.
x 10^5
2.5
2
1.5
1
0.5
0
Alt. (ft)
0
5
10
15
20
25
Mach No.
Bank
No Bank
Chattering

Figure 9

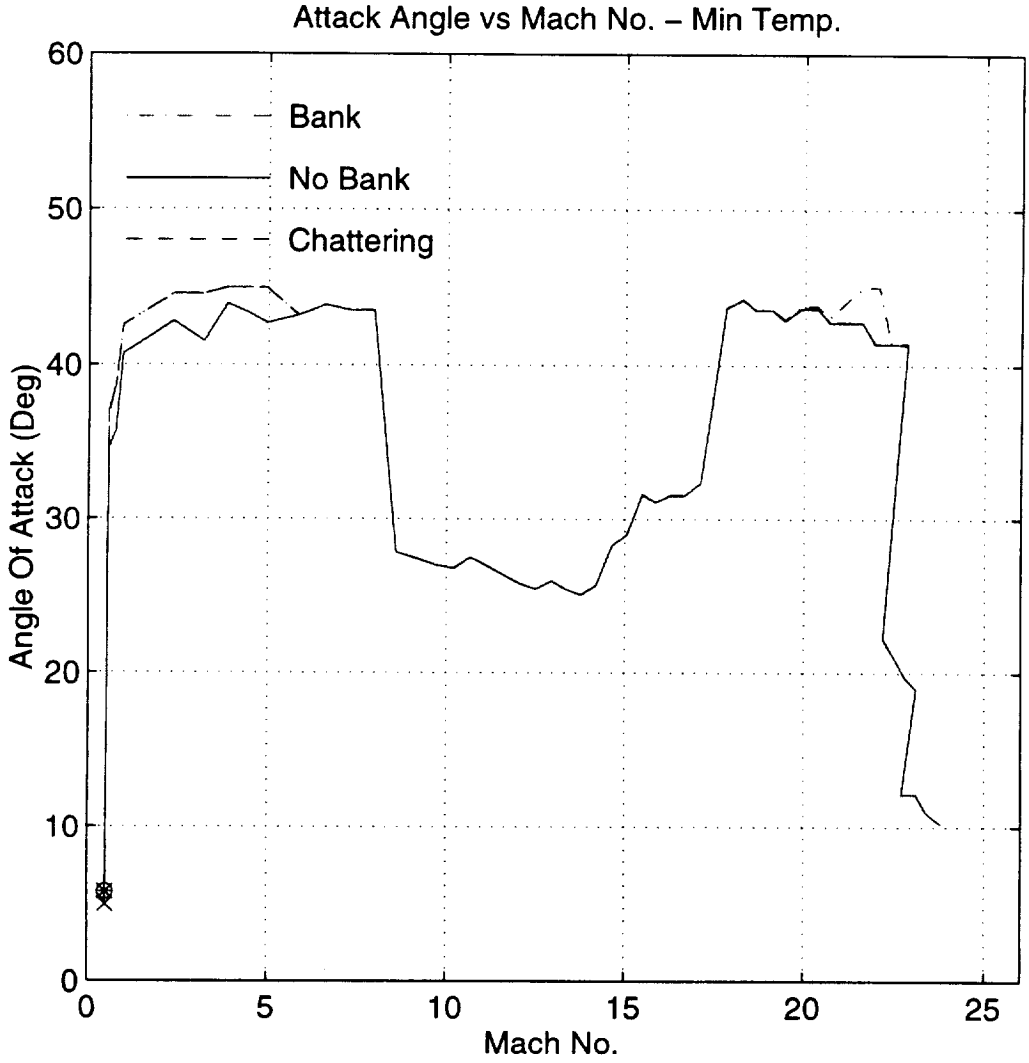
Attack Angle vs Mach No. – Min Temp.
Bank
No Bank
Chattering
Angle Of Attack (Deg)
Mach No.
0
10
20
30
40
50
60
0
5
10
15
20
25

Figure 10

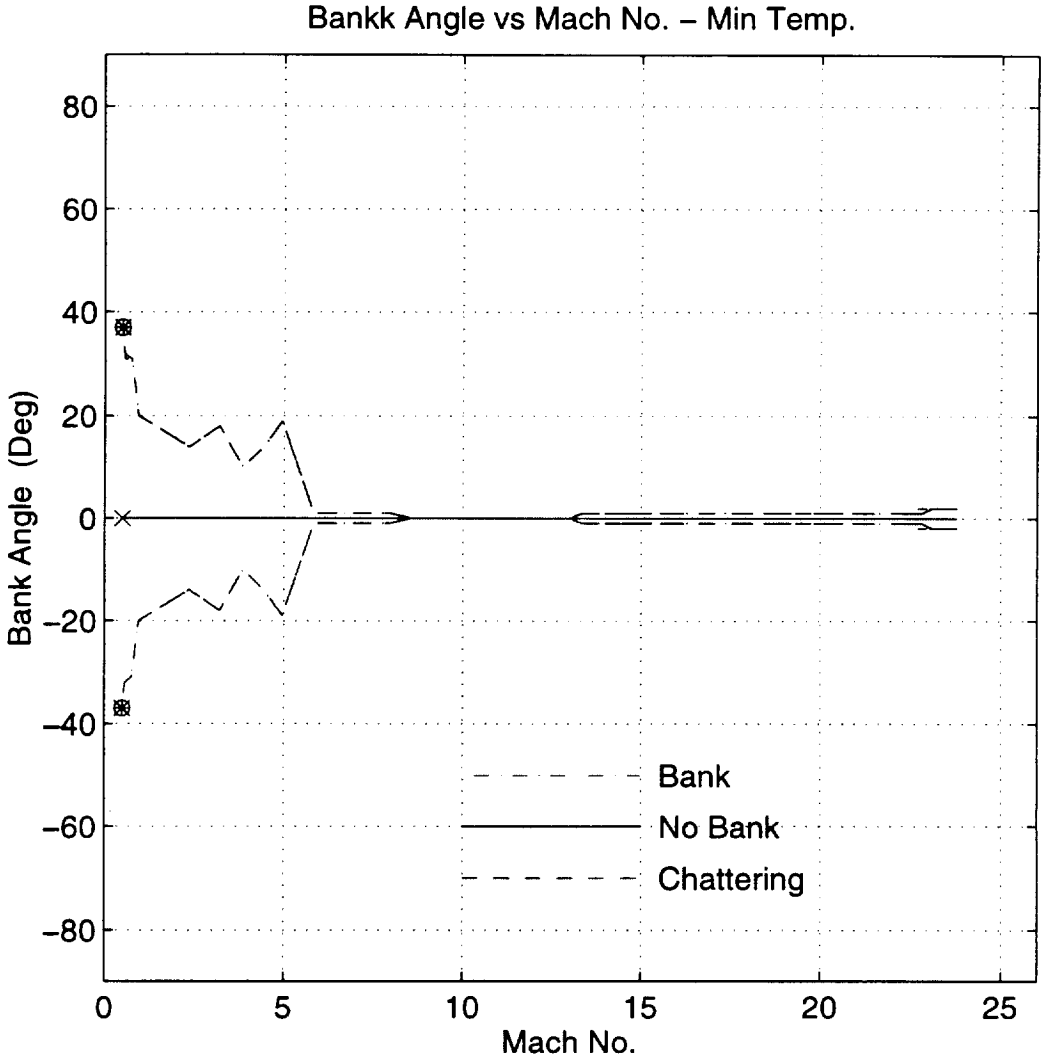
Bankk Angle vs Mach No. – Min Temp.
Bank Angle (Deg)
Mach No.
80
60
40
20
0
−20
−40
−60
−80
0
5
10
15
20
25
Bank
No Bank
Chattering

Figure 11

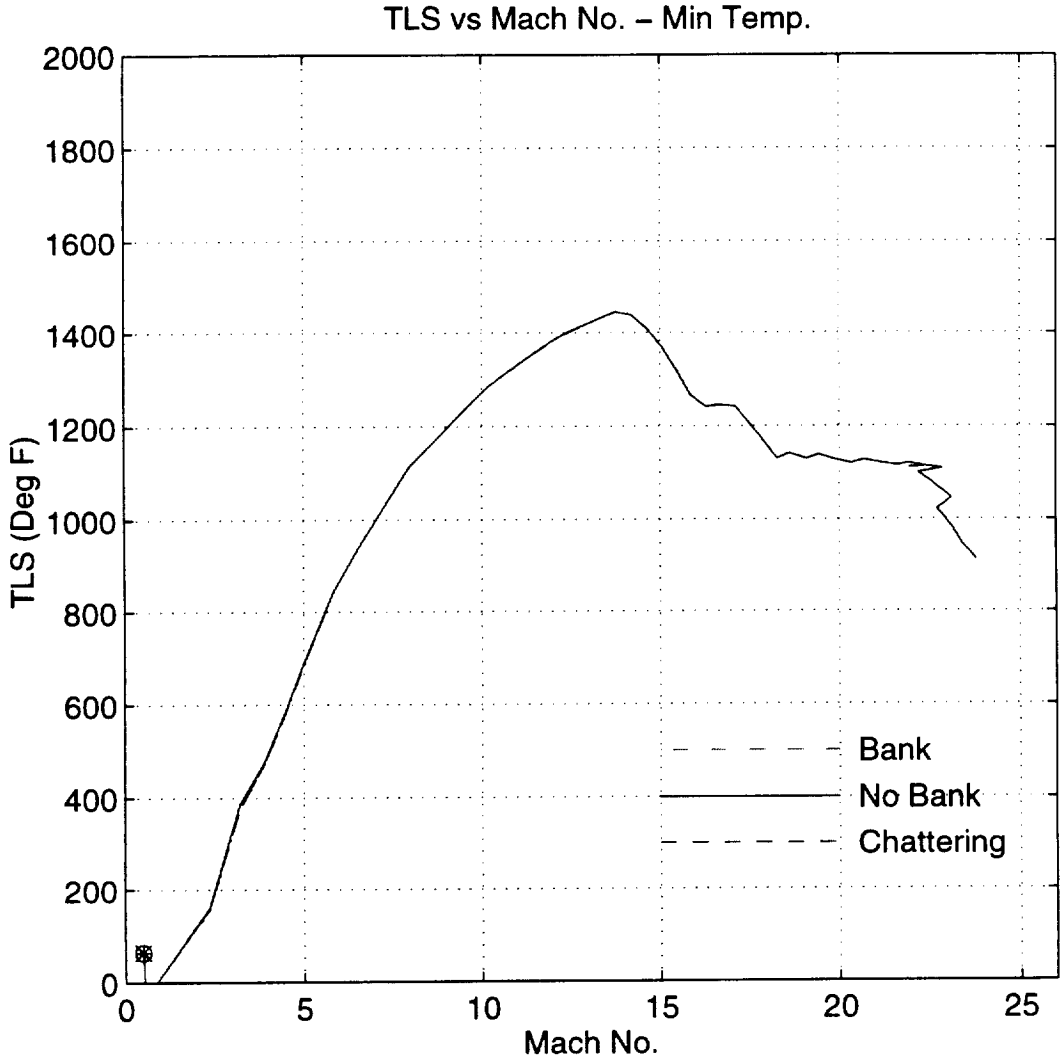
TLS vs Mach No. – Min Temp.
TLS (Deg F)
Mach No.
2000
1800
1600
1400
1200
1000
800
600
400
200
0
0
5
10
15
20
25
Bank
No Bank
Chattering

Figure 12

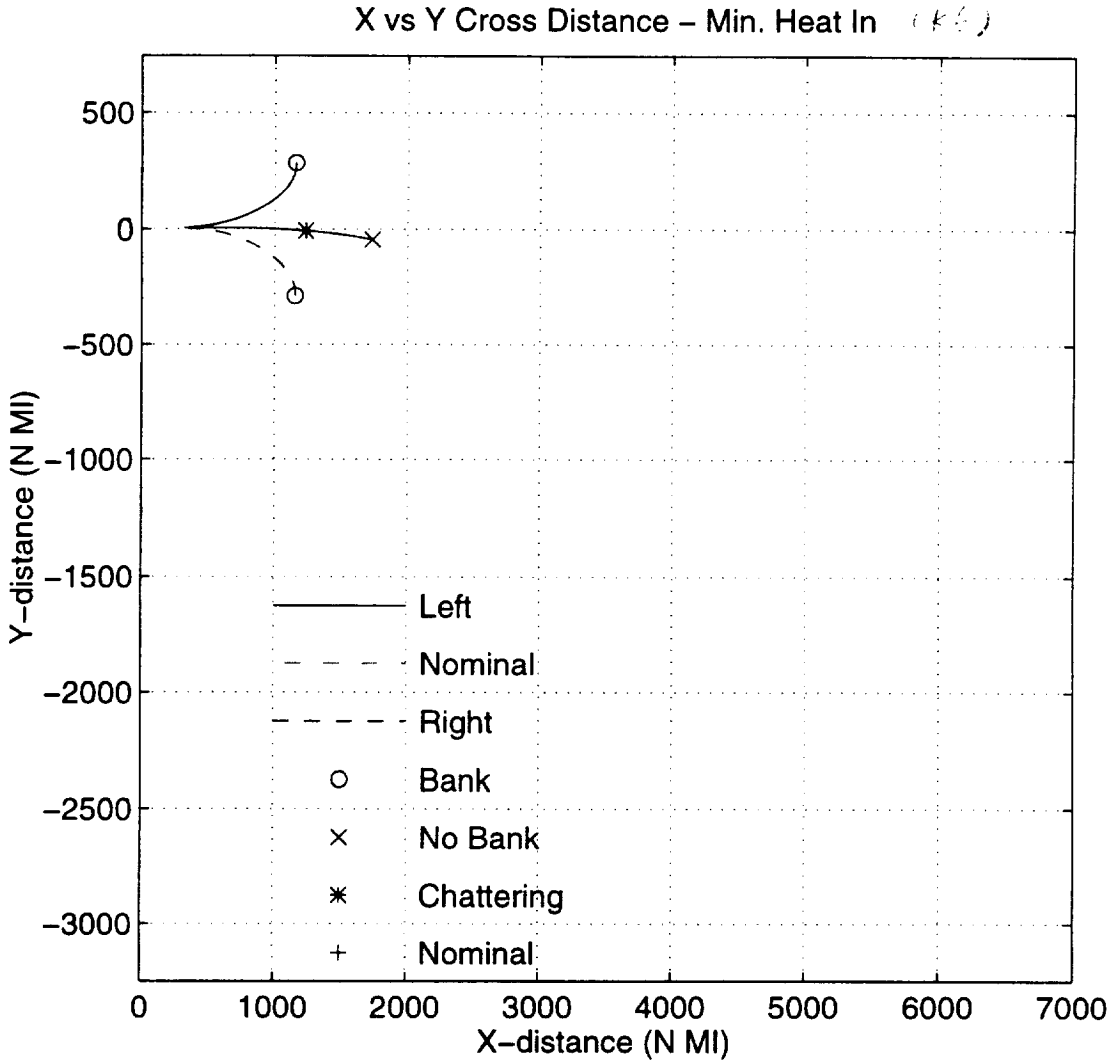
X vs Y Cross Distance – Min. Heat In
500
0
−500
−1000
−1500
−2000
−2500
−3000
Y−distance (N MI)
0
1000
2000
3000
4000
5000
6000
7000
X−distance (N MI)
Left
Nominal
Right
Bank
No Bank
Chattering
Nominal

Figure 13

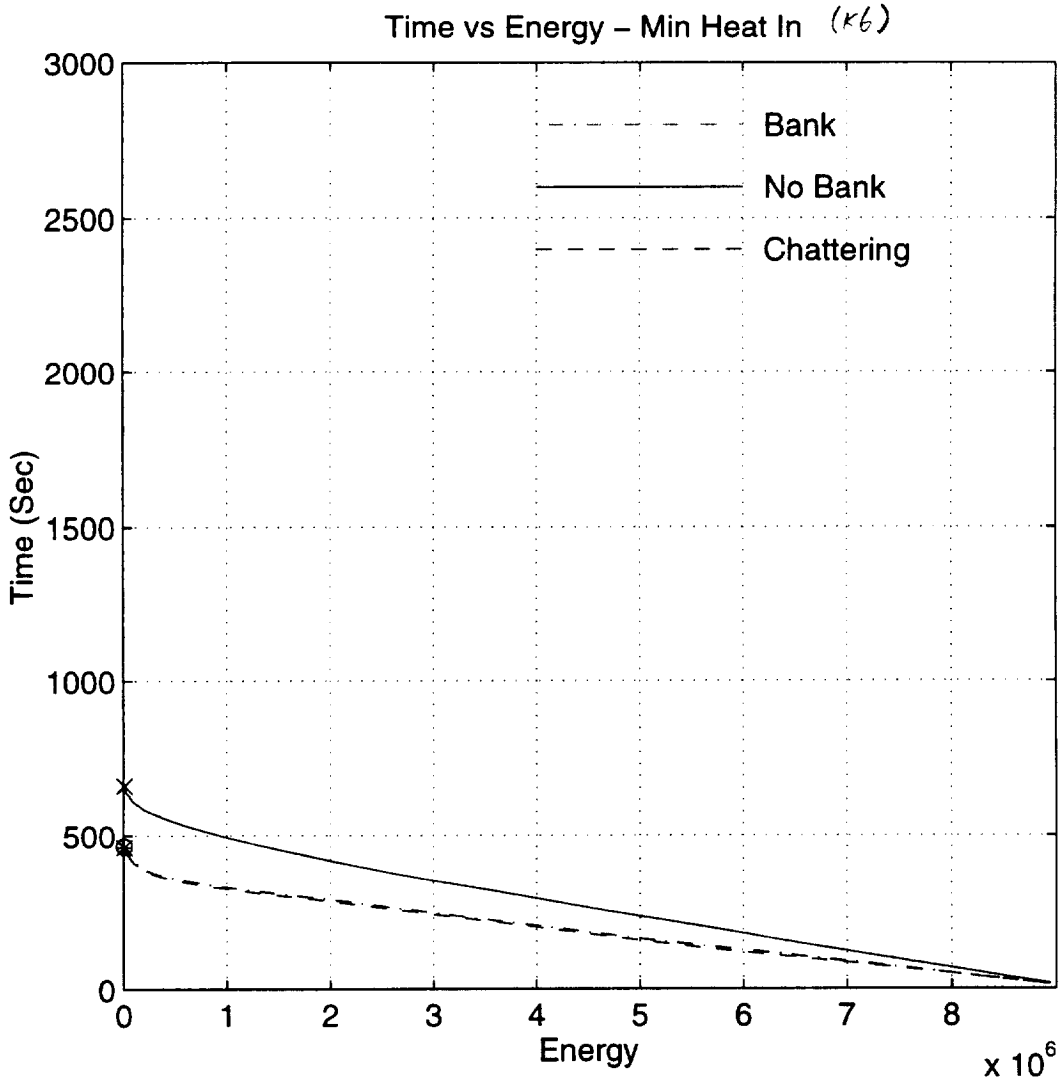
Time vs Energy – Min Heat In (K6)
Bank
No Bank
Chattering
Time (Sec)
Energy
x 10^6
3000
2500
2000
1500
1000
500
0
0
1
2
3
4
5
6
7
8

Figure 14

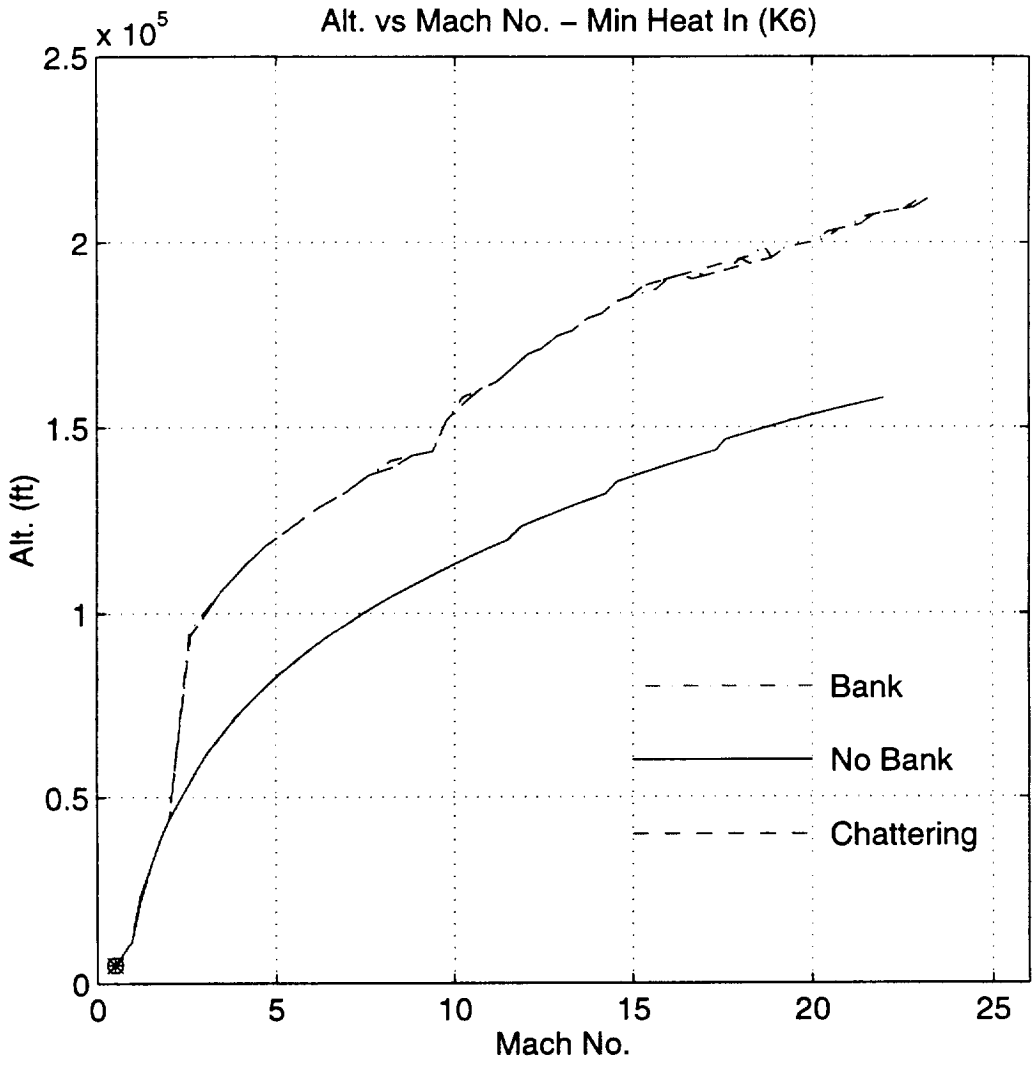
Alt. vs Mach No. – Min Heat In (K6)
x 10^5
2.5
2
1.5
1
0.5
0
Alt. (ft)
0
5
10
15
20
25
Mach No.
Bank
No Bank
Chattering

Figure 15

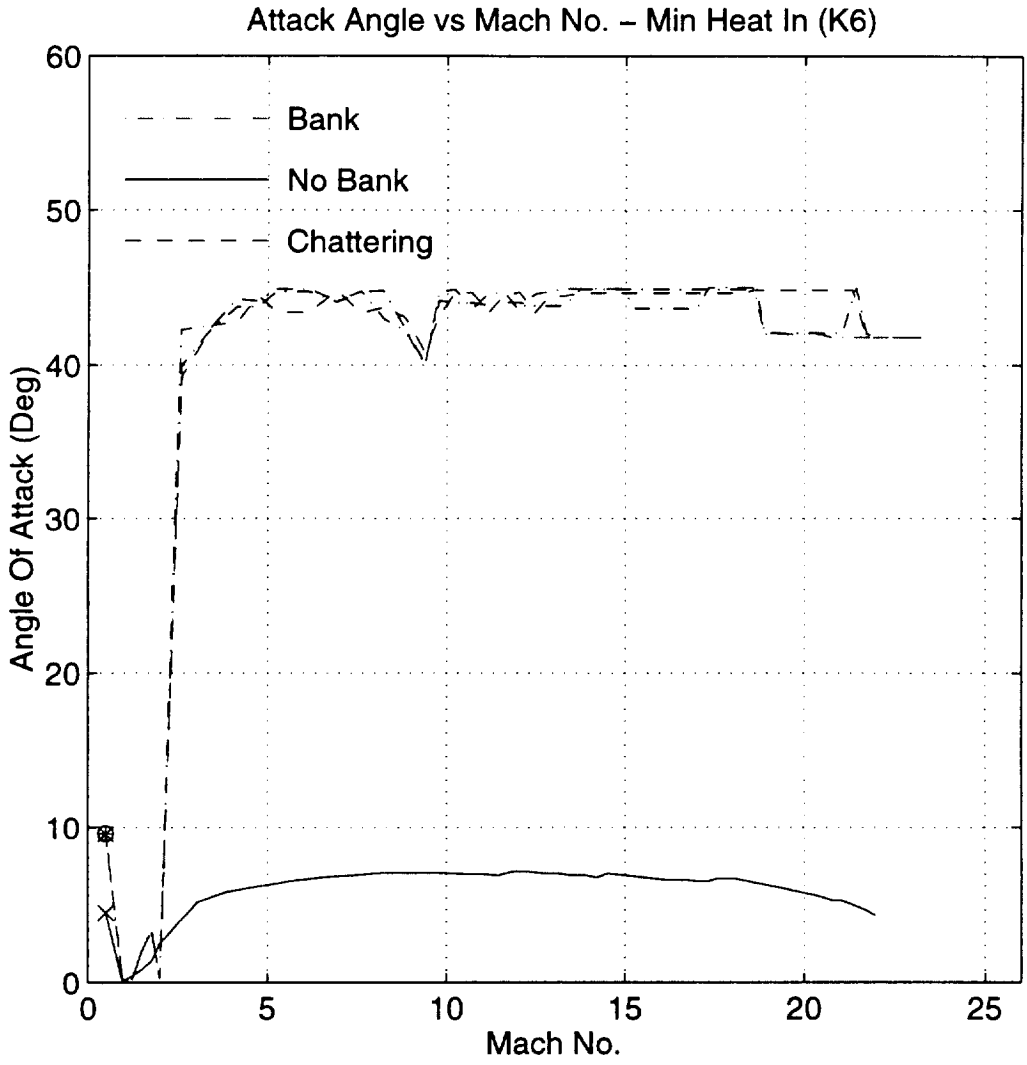
Attack Angle vs Mach No. – Min Heat In (K6)
Bank
No Bank
Chattering
Angle Of Attack (Deg)
Mach No.
0
10
20
30
40
50
60
0
5
10
15
20
25

Figure 16

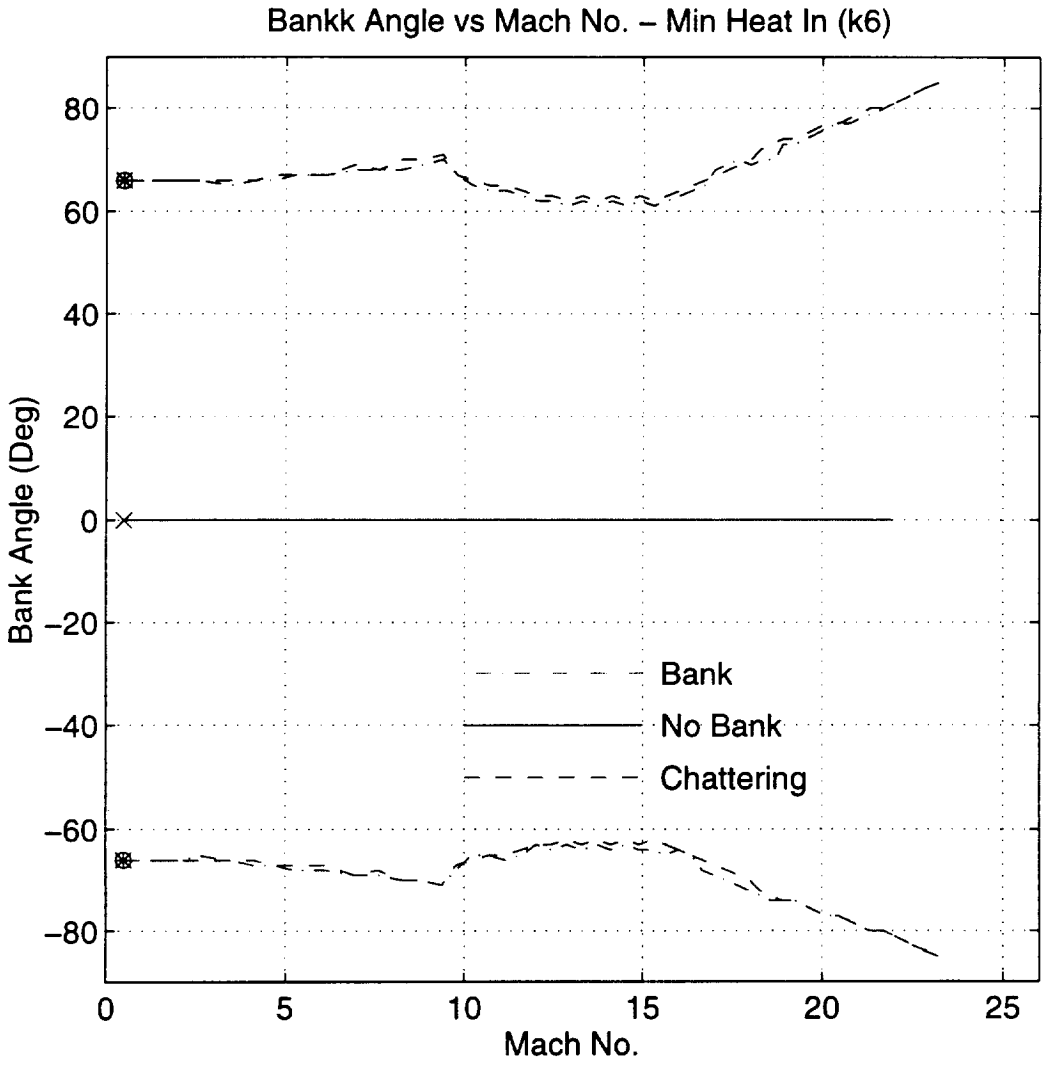
Bankk Angle vs Mach No. – Min Heat In (k6)
Bank Angle (Deg)
80
60
40
20
0
−20
−40
−60
−80
0
5
10
15
20
25
Mach No.
Bank
No Bank
Chattering

Figure 17

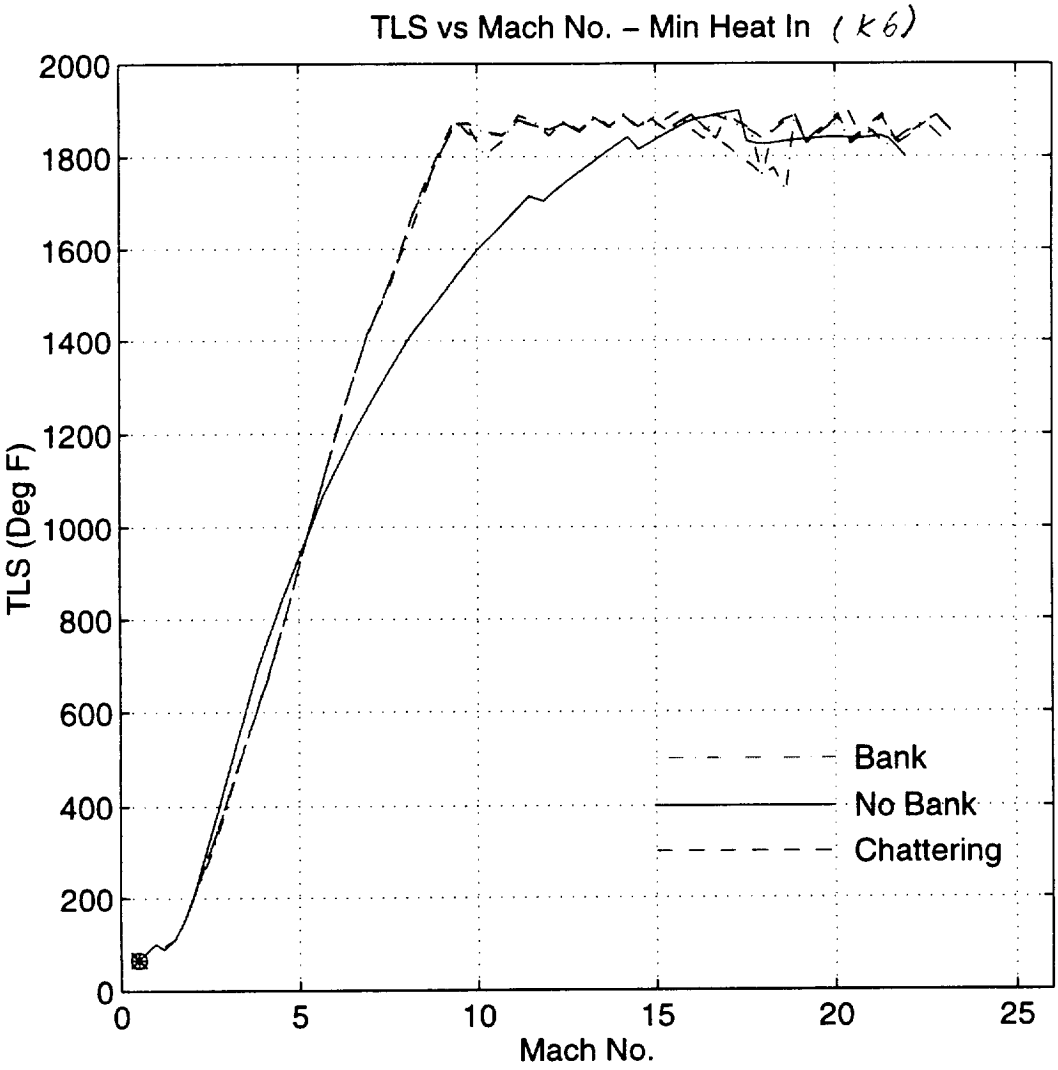
TLS vs Mach No. – Min Heat In (k6)
TLS (Deg F)
Mach No.
2000
1800
1600
1400
1200
1000
800
600
400
200
0
0
5
10
15
20
25
Bank
No Bank
Chattering

Figure 18

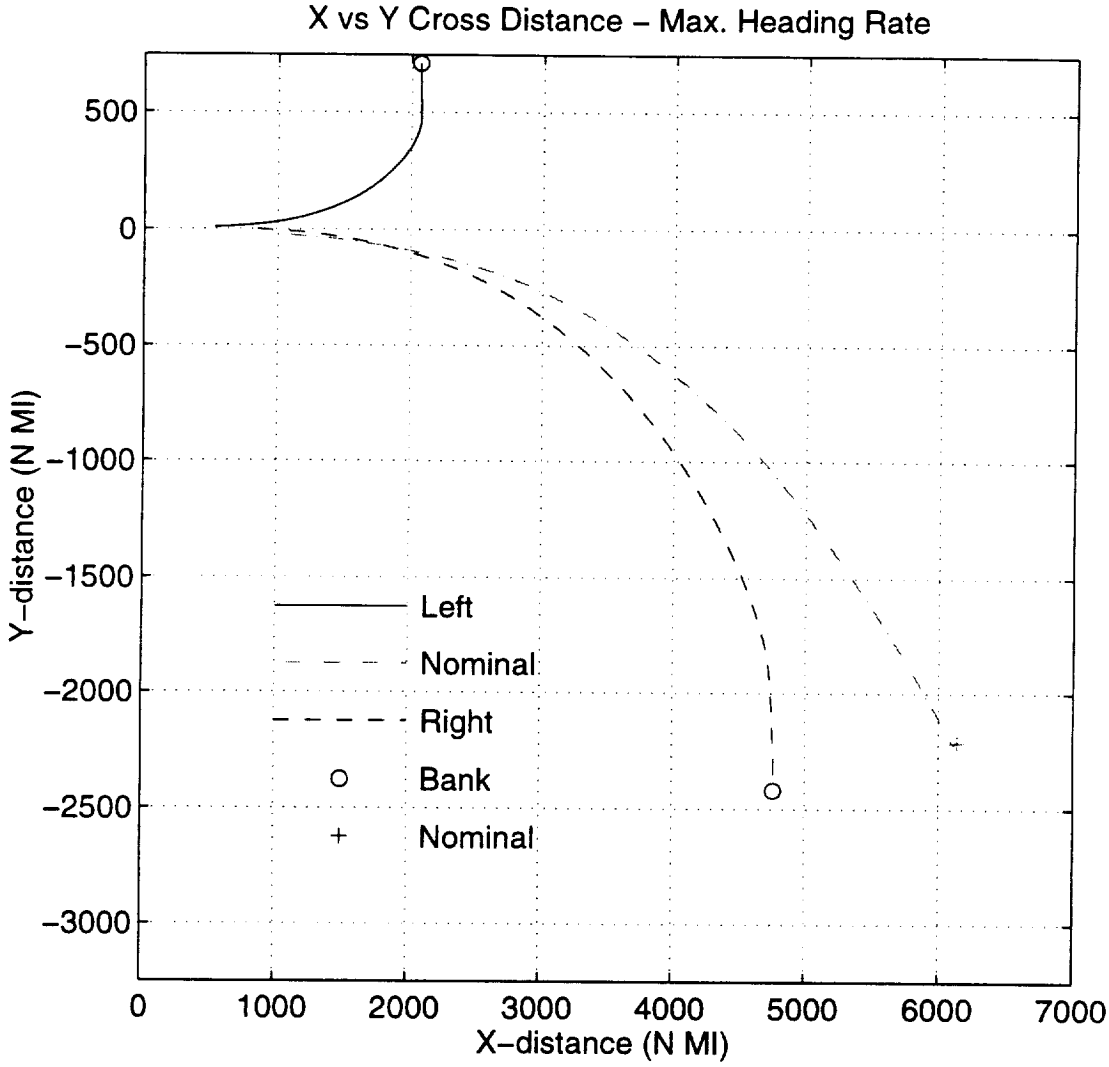
X vs Y Cross Distance – Max. Heading Rate
500
0
-500
-1000
-1500
-2000
-2500
-3000
Y-distance (N MI)
0
1000
2000
3000
4000
5000
6000
7000
X-distance (N MI)
Left
Nominal
Right
Bank
Nominal

Figure 19

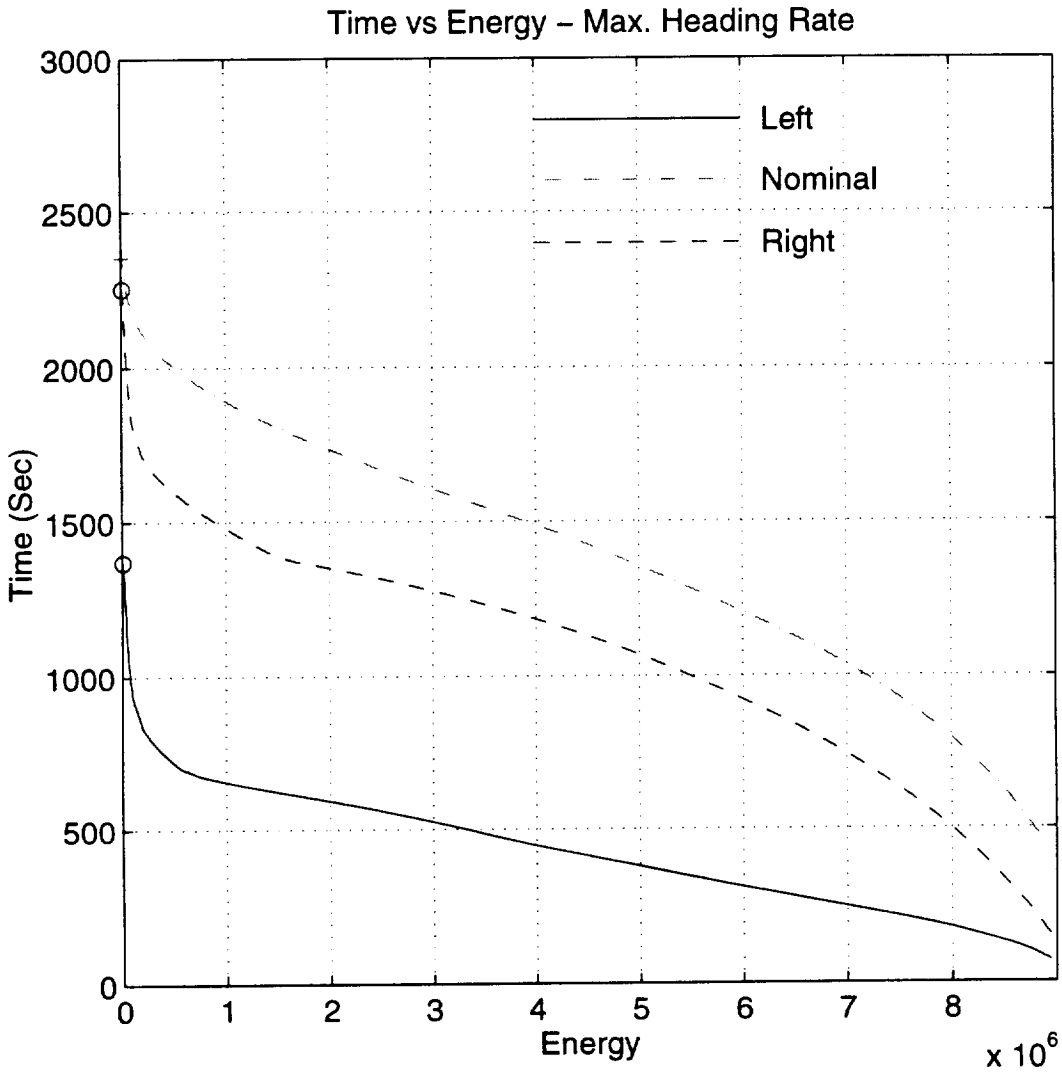
Time vs Energy – Max. Heading Rate
Left
Nominal
Right
Time (Sec)
Energy
x 10^6
3000
2500
2000
1500
1000
500
0
0
1
2
3
4
5
6
7
8

Figure 20

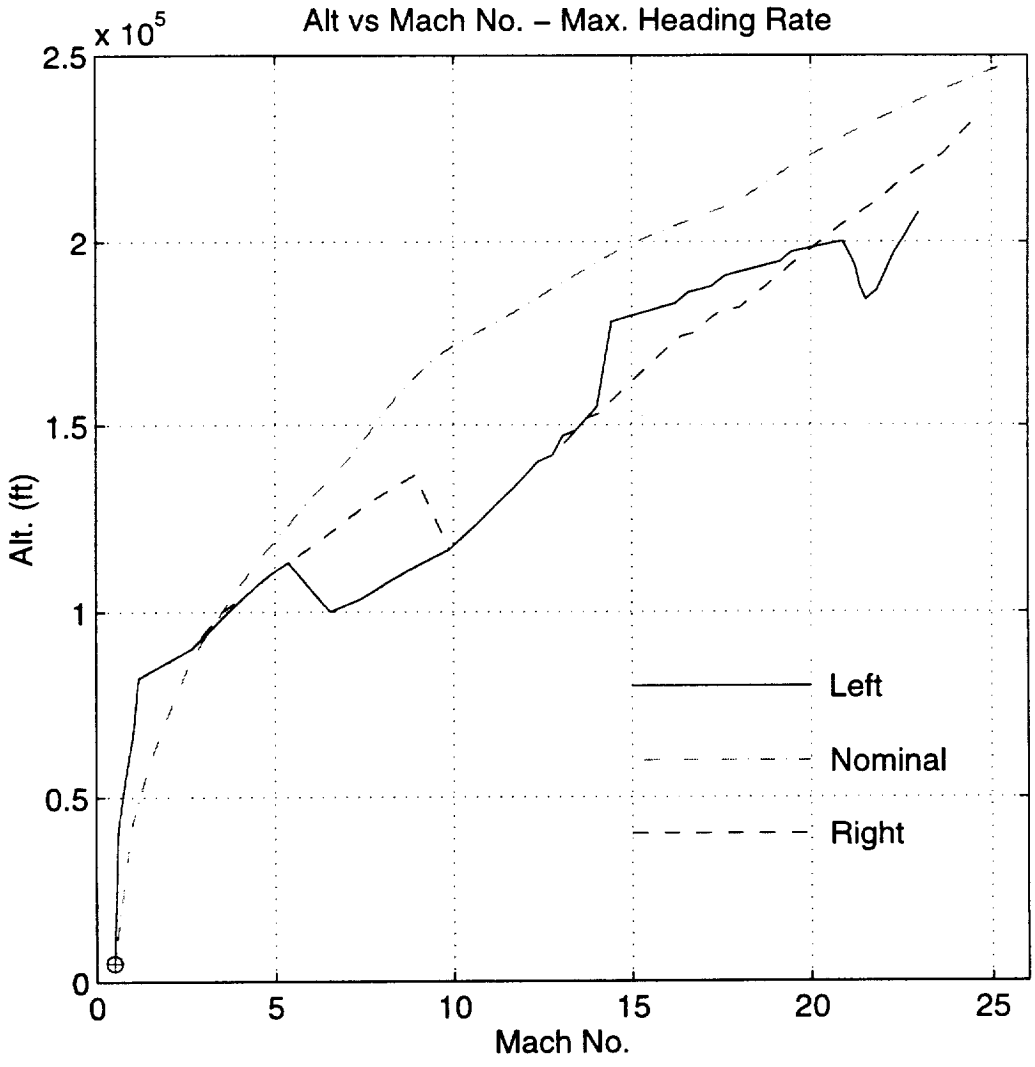
Alt vs Mach No. – Max. Heading Rate
x 10^5
2.5
2
1.5
1
0.5
0
Alt. (ft)
0
5
10
15
20
25
Mach No.
Left
Nominal
Right

Figure 21

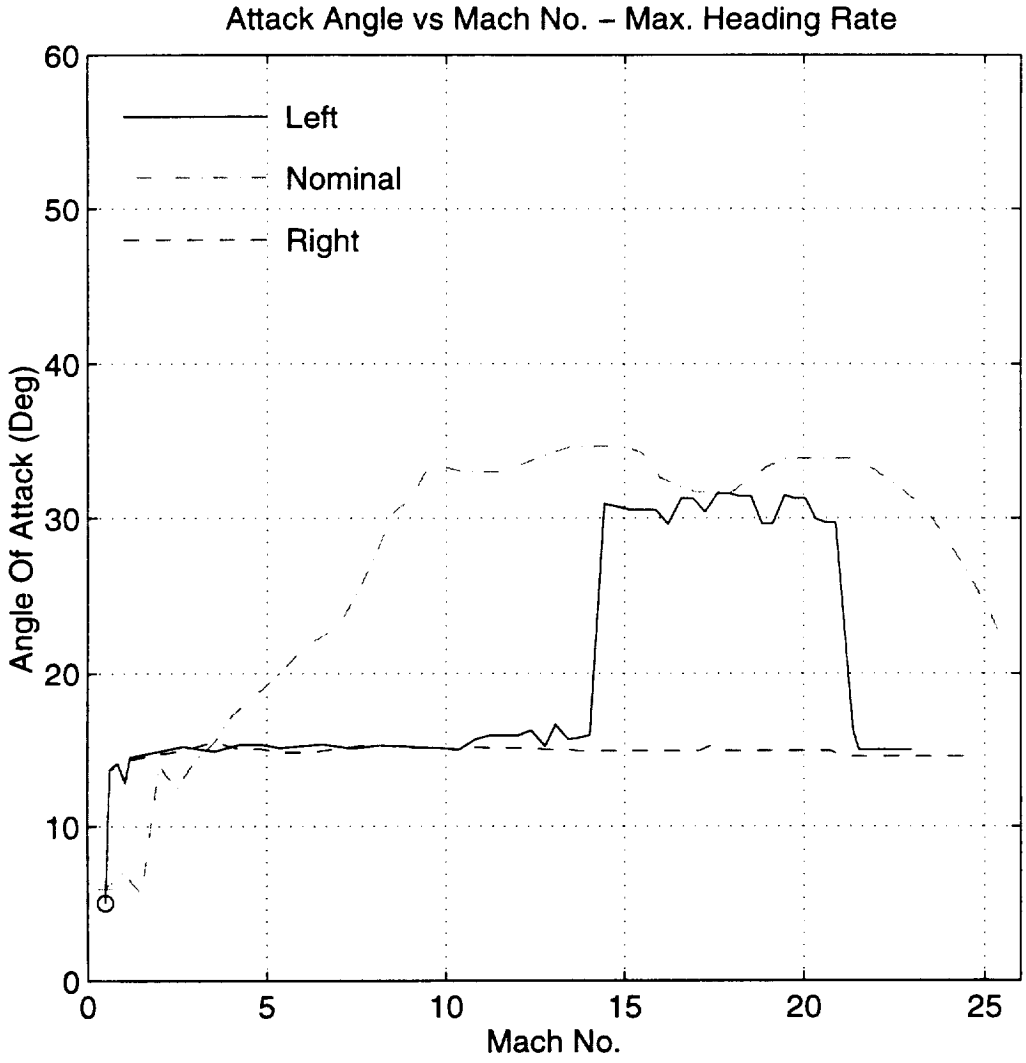
Attack Angle vs Mach No. – Max. Heading Rate
Left
Nominal
Right
Angle Of Attack (Deg)
Mach No.
0
10
20
30
40
50
60
0
5
10
15
20
25

Figure 22

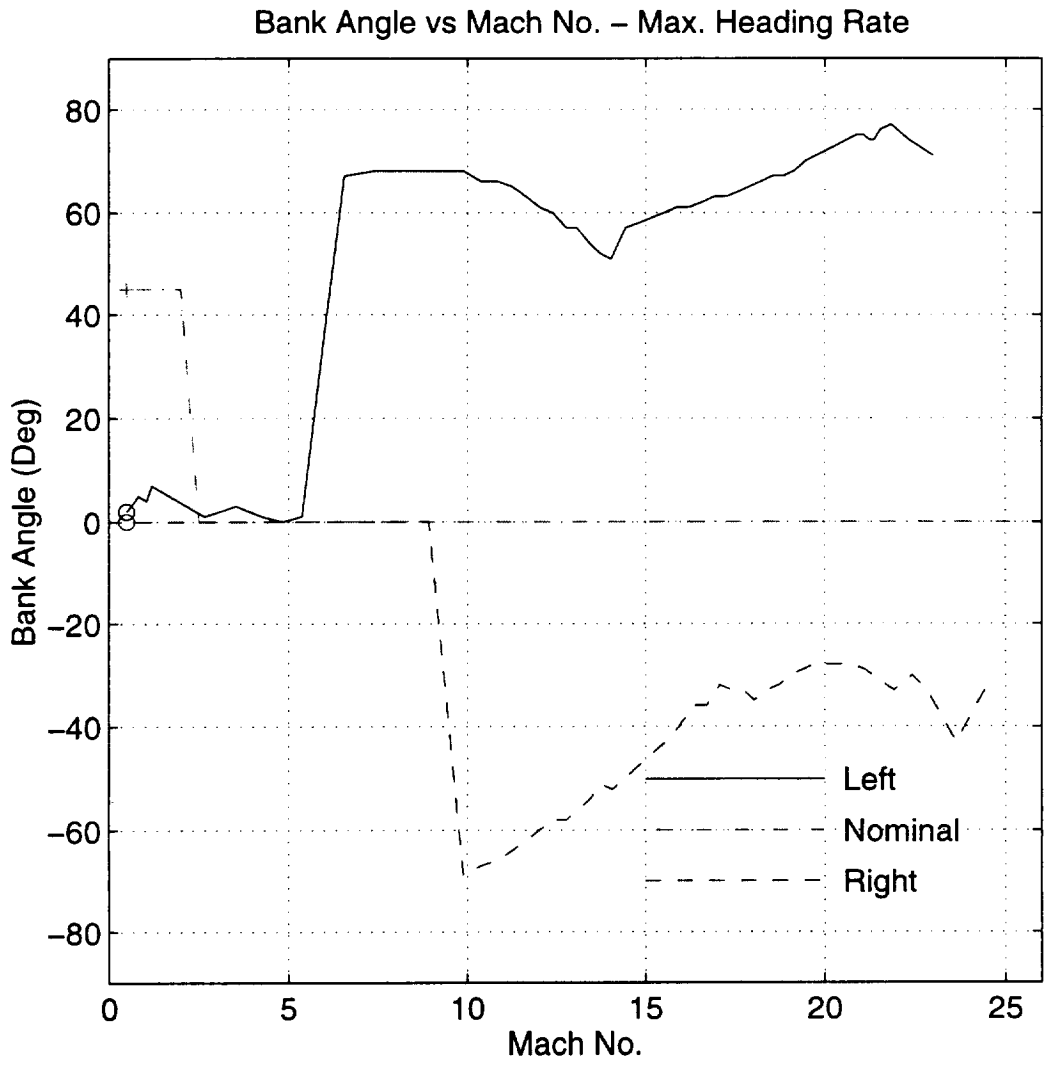
Bank Angle vs Mach No. – Max. Heading Rate
Bank Angle (Deg)
80
60
40
20
0
−20
−40
−60
−80
0
5
10
15
20
25
Mach No.
Left
Nominal
Right

Figure23

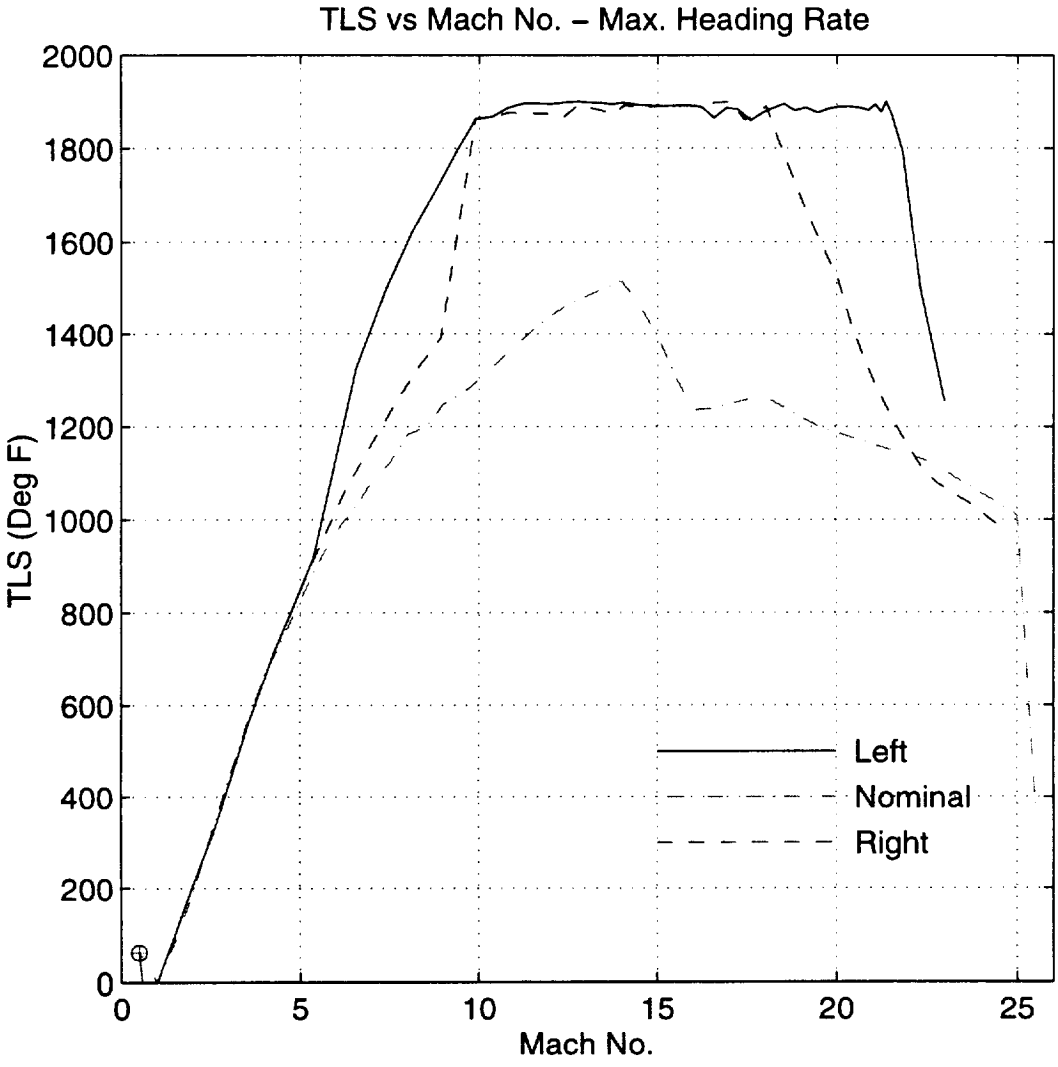
TLS vs Mach No. – Max. Heading Rate
TLS (Deg F)
Mach No.
2000
1800
1600
1400
1200
1000
800
600
400
200
0
0
5
10
15
20
25
Left
Nominal
Right

Figure 24

Appendix A

Near-Optimal Operation of Dual-Fuel Launch Vehicles

by

M. Ardema, H. Chou, J. Bowles

AIAA Paper 96-3397

Presented at

AIAA Atmospheric Flight Mechanics Conference

San Diego, CA

July 29 - 31, 1996

APPENDIX B

Composite Material Structural Weight Estimation

by

L. Hornberger, M. Ardema, and F. Dickerson

COMPOSITE MATERIAL STRUCTURAL WEIGHT ESTIMATION

by
Mark Ardema, Frank Dickerson and Lee Hornberger
Mechanical Engineering Department
Santa Clara University

ADDING COMPOSITES TO HAVOC

Light weight materials such as fiber reinforced plastics (composites) and bonded honeycomb sandwiches have become more and more common in airplanes in the last two decades (1). Designers value the unique properties of these materials, particularly their high stiffness to weight ratios. They must, however, balance these assets against the additional cost of these materials and their manufacture. To aid designers with this analysis, a composites subroutine has been added to the HAVOC structures weight calculation code. This subroutine sizes the thickness of a particular composite necessary to withstand the required aircraft loads, and provides this information to HAVOC which calculates the resultant weight of the aircraft.

TYPICAL AIRCRAFT COMPOSITES

The selection and use of composites on transport aircraft is an evolving process. A variety of composites have been tested in both military and commercial aircraft in the last 25 years (1). These composites typically consist of a strong, stiff fiber such as glass, graphite or kevlar, and a protective, adhering, inexpensive plastic matrix such as polyester or epoxy.

Glass fibers embedded in a polyester matrix have been the dominate composite for military and civil aircraft in the past. Currently, the aircraft industry prefers the stiffer and higher temperature composites made from carbon fiber in an epoxy matrix. However, the grade of carbon fiber and epoxy seems to change from year to year and from airplane manufacturer to airplane manufacturer. The current favored carbon fibers are AS4 (Hercules/Hexcel), IM6 and IM7 (Hercules/Hexcel) . The AS4 is an economical, high-strength carbon fiber and the IM6 &7 are high-modulus expensive fibers. These three carbon fibers have been used on military

aircraft and in research, but are not on commercial vehicles. The T-800 fiber (a Toray equivalent to IM7) has recently been used in some commercial applications (1-6).

Epoxies, particularly the 350°F curing systems, are the least expensive high temperature options for matrix materials. Several epoxy systems have been developed and tested for use with specific fibers. There is a current trend to use rubber modified epoxies such as 8552 and 3900 to increase the toughness of the composite system and its resistance to impact. Fiber-resin combinations currently in use by airplane designers and researchers are:

AS4/938 (ICI Fiberite) -Boeing Advanced Composites Program Door Panel(2)
AS4/8552 (Hexcel/Hercules), -Boeing Adv. Comp Fuselage (6-7)
AS4/8551 (Hexcel/Hercules) (6)
AS4/3501-6 (Hercules) -McDonnell Douglas Adv. Technology Composite Wing program (8)
AS4/3502 (Hercules) Military Aircraft (6)

COMPOSITE STRUCTURAL ANALYSIS

Composite materials were originally added to the options in the HAVOC program in 1995. This was done by simulating these materials by homogeneous structures with uniform mechanical properties (strength and modulus of elasticity) in every direction. This approach limits the code to evaluation of only the simplest and weakest type of composites called random mat[1]. Random mat composites are made by stacking the reinforcing fiber in all direction throughout the thickness of the material. In this type of composite the elastic properties and strength of the layup are roughly the same in every direction but the fiber density and reinforcement is low in any specific direction.

Random mat composites are not favored by aircraft designers because of their low strength to weight ratios. The preferred type of composite for these applications are ones in which the properties of the material are customized to meet the specific directions and magnitudes of the

---

1 See Appendix A for definition of composite terms

structural loads. This yields the minimum weight composite for the job. To accomplish this, composite designers specify a layup pattern for a composite laminate relative to a major axis of loading.

A typical composite laminate is made of a stack of 4-16 plys. A ply is a single layer of parallel reinforcing fibers embedded in a partially cured matrix of plastic. The location of each ply in the stack is defined relative to the angle its fibers makes with a major axis, such as the x-axis. For instance. a 0/90/90/45/0 layup is one in which the fibers of the outer and inner layers are parallel to the x-axis, the next two plies have fibers perpendicular to this axis and the fibers of the third layer are at an angle 45° clockwise to the x axis. This type of composite would have reinforcing fibers to sustain tensile and compressive loads in the x and y directions but would be weakest in the 45° direction. Composites walls for structural parts such as aircraft are often made from stacks of these laminates.

Analysis of a multilayer stack is more complex than that of homogeneous materials such as aluminum or random mat and requires the use of a macromechanics approach to determine elastic properties and strength. The macromechanics approach used in the COMPOS part of the HAVOC code is that presented in most textbooks on composite design (9-11) . In this approach the stiffness of a particular laminate is calculated by summing the contributions of each layer (ply) in the stack to the stiffness of the laminate in a particular direction. The composite stiffness in each major direction is then used to calculate the net strain of the composite in that direction due to the applied loads. From the net strain, the strain on each layer (ply) parallel and transverse to its fiber is derived. The resulting strains are then compared to the failure strains of the ply material and from this the potential for the failure of the stack is determined. The details of implementing this approach in HAVOC are described in the following section describing the COMPOS (composites) code addition.

COMPOS CODE

COMPOS is a section of code which has been added to HAVOC program to calculate the minimum laminate thickness required to withstand the forces imposed at each section of the airplane.

Assumptions within COMPOS

•The laminate is symmetric and orthotropic. (This type of layup is commonly used in aircraft design to minimize warpage of the layup).
• Every ply in the stack is composed of the same resin- fiber material.
• The stack is a minimum of 3 plys. (A ply is usually .003-.007 inches thick depending on the material.)
• The modulus of the material is the same in compression and tension. (if the compression modulus is different than its tensile modulus, the smaller of the two values is selected for all calculations.)
• Failure of the composite laminate occurs when any single ply fails.
• Failure of a ply occurs when it reaches the maximum strain transverse or parallel to the fiber direction in tension, compression or shear (11) Maximum strain theory is invoked in this analysis because it is currently believed to be the most predictive failure theory for composites (3,4,8) .
•The minimum gage thickness for the composite material is assumed to be the thickness of the initial laminate (a stack of plies).
•All loads are applied in the plane of the ply. This means that there are no z direction loads in tension, compression or shear.
• The buckling equations used in HAVOC to analyze the frames and stringers made from homogeneous materials apply to these heterogeneous materials. For buckling analysis the modulus of the laminate in the direction of load is used. This is a very course assumption and may*be somewhat optimistic for quasi isotropic composites manufactured with adhesive joints but seems highly unlikely for symmetric orthotropic laminates with heterogeneous properties. However, buckling analysis of complex composites structures is still in the developmental stage.(12)*

Calculation Procedure

•Calculations for Compressive and Tensile Loads
Once the maximum tensile and/or compressive loads per unit width (Nx and Ny) at any given aircraft section are determined in the HAVOC code, they are transferred to the COMPOS subroutine. The effect of these normalized forces on the composite laminate strain is calculated using the following relationship for an orthotropic symmetric laminate (9) :

$$[N] = [A] \times [\varepsilon^0] \qquad (1)$$

Where:

[N] = Matrix of forces on the composite section (Nx, Ny and Nxy)
[A] = Stiffness matrix of the composite
$[\varepsilon^0]$ = strain matrix of the composite (ex, ey, exy)

The components of the stiffness matrix [A] are determined in the code through the following relationship (9):

$$A_{ij}=\Sigma^{n}_{\kappa=1}(QB_{ij})_k(h_k) \qquad (2)$$

Where:

QB_{ij} = component of each ply's stiffness in the i and j's directions
h = thickness of k ply
k= ply number in the laminate

The stiffness contributions, QB values, of each ply are determined from the initial ply properties, E1, E2, ν_{12} and the ply angles, θ, specified by the user in the input file for a particular laminate construction. (Here, the "1" direction is taken parallel to the fiber and the "2" direction transverse to the fiber).

Once the average laminate strain is determined from equation (1), this strain is then transferred to each ply and transformed into strain parallel and transverse to each fiber as well as shear strain. These strains are then divided by the mating failure strains for the material (supplied by the user in the input file) to determine the R value of the layup.

$R_{ij}= alle_{ij}/e_{ij}$

Where:

$alle_{ij}$=allowable components of strain in principle ply direction
e_{ij} = components of strain in principle ply directions

If the R value for all plys in all the principle directions is more than 1, the laminate thickness is adequate to support the load and is left unaltered. If R is less than one on any ply in any of the principle directions, the thickness of the laminate is increased by giving it the value of it initial thickness divided by R.

Calculations for Buckling

HAVOC currently determines critical buckling loads from the modulus of elasticity of the material. COMPOS calculates the modulus of the laminate in the direction parallel to the buckling force and passes this value back to HAVOC. As mentioned in the assumptions portion of this report, the buckling calculation of HAVOC may not be valid for composites as they were developed for isotropic materials. *Little research has been done on composites in buckling so the authors advise caution in interpreting this result particularly with non-isotropic layups.*

NON-OPTIMUM FACTORS

Unfortunately, few all composite planes have been built so it is difficult to find planes to use as checks for the composite section of the code (8). The all composite planes listed in the literature (8) are:

- Windecker Eagle in 1967 which was glass fiber reinforced
- Learfan in 1981 which used glass, carbon and kevlar fibers
- Piaggio Avanti in 1986 with carbon fiber parts
- Beech Starship in 1986 with carbon fiber
- Grob GF-200- all composite
- Slingsby T-3A Firefly -all composite

A literature search and personal interviews failed to turn up much information directly useful in determining non-optimum factors. (These factors are used to multiply the results of theoretical calculations to get weights of practical structures.)

One reference was found which had this type of data (12). In this reference, a theoretical analysis gave 8640 pounds as the weight of a composite wing box whereas the actual wing was estimated to weigh 11,284 pounds giving a non-optimum factor of 1.306. Using the non-optimum factors for aluminum structures (13) this number can be used to estimate non optimum factors for carbon fiber-epoxy structures. If it is assumed that the non-optimum factors for the fuselage primary structure increase in the same proportion as wing structure relative to aluminum, and that the increments for secondary structure and non-structural are the same for graphite-epoxy composites and aluminum, then the following non-optimum factors for the composite result:

	Primary Structure	*Primary &Secondary Structure*	*Total Assembly*
Fuselage	1.792	2.329	3.010
Wing	1.306	1.666	2.059

There are many composite components in commercial and military structure as well as some from research on advanced composites. It may be possible to compare these components to predictions of the code.

REFERENCES

1. Vosten, L. F., "Composite Chronicles: Past Performance and Future Prospects," Fourth NASA/DoD Advanced Composites Technology Conference, 1993, Salt Lake City, Utah, vol 1. p 1

2. Russell, S., Vastava, R., Ley, R., Polland, D and Mabson, G., "Design Cost Modeling of Fuselage Door Cutout Structure," Fifth NASA /DoD Advanced Composites Technology Conference August 22-25 1994. NASA Conference Publication 3294 Volume I, Part I. p 127.

3. Personal communication from Professor. Steve Swanson, Univ of Utah, Mechanical Engineering Department

4. Personal communication from Professor Mark Tuttle, Univ of Washington, Mechanical Engineering Department

5. Personal communication from George Lallas of Hexcel/Hercules

6. Personal communication from Jim Stearns of NASA Langley

7. Scholz, D., et al, "Material and Processing Development for Composite Fuselage Sandwich Structure," Fifth NASA /DoD Advanced Composites Technology Conference August 22-25 1994. NASA Conference Publication 3294 Volume I, Part I. p 257.

8. Hawley, A.V., "Preliminary Design of a Transport Aircraft Composite Wing, " Fifth NASA /DoD Advanced Composites Technology Conference August 22-25 1994, proceedings of which are contained in NASA Conference Publication 3294 Volume I, Part I,p. 736

9. Jones, R., *Mechanics of Composite Materials,* McGraw-Hill, New York, 1975.

10. Tsai, S., *Composite Design*, 4th edition, THINK COMPOSITES, Dayton, 1988.

11. Agarwal, B., and Broutman, L., *Analysis and Performance of Fiber Composites*, 2nd ed., John Wiley and Sons, New York. 1990.

12. Swanson, G., Wishart, R and Eastland, C, "Compression Test Results for Stiffened Composite Fuselage Structure," Fourth NASA /DoD Advanced Composites Technology Conference June 7-11 1993, Salt Lake City, Utah NASA Conference Publication 3229 Volume I, Part I, p125.

13. Ardema, M.D. et al., "Analytical Fuselage and Wing Weight Estimation of Transport aircraft, NASA TM 110392, May 1996.

APPENDIX 1
COMPOSITES TERMINOLOGY

Random Mat- equal fibers in every direction
Balanced- equal fibers in orthotropic directions yield a composite with identical properties in 2 principal directions.
Symmetric-A symmetric laminate is one in which for each ply above the center of the stack there is and identical one at an equal distance below the center. For instance, a 0/-45/90/90/-45/0 is a symmetric layup but a 0/-45/90/ 0/-45/90 is not.
Quasi-Isotropic- Layups which are designed to have only two independent elastic constants, the modulus of elasticity and Poisson's ratio. These materials have the same values in every inplane direction. To meet this criteria fiber (ply) layups must have the following conditions:

- Total number of plies must be 3 or more
- Individual plies must have identical stiffness [Q] matrices and thickness
- Layers must be oriented at "equal" angles (if total number of layers is n, than each layer is pi/n relative to the next). If the laminate is constructed from several groups of laminates,. the condition must be satisfied for each laminate group

Typical laminates which satisfy these rules : [0/60/-60], [0/45/-45/90]